

## HMA1, a new Cu-ATPase of the chloroplast envelope, is essential for growth under adverse light conditions

Daphné Seigneurin-Berny<sup>a,\*</sup>, Antoine Gravot<sup>b,\*</sup>, Pascaline Auroy<sup>b</sup>, Christophe Mazard<sup>a</sup>,  
Alexandra Kraut<sup>a</sup>, Giovanni Finazzi<sup>c</sup>, Didier Grunwald<sup>d</sup>, Fabrice Rappaport<sup>c</sup>, Alain  
Vavasseur<sup>b</sup>, Jacques Joyard<sup>a</sup>, Pierre Richaud<sup>b</sup> and Norbert Rolland<sup>a</sup>

From the <sup>a</sup> Laboratoire de Physiologie Cellulaire Végétale, UMR 5168 CNRS/CEA/INRA/Université Joseph Fourier, DRDC/CEA-Grenoble, 17 rue des Martyrs, 38054 Grenoble-cedex 9, France. <sup>b</sup> Laboratoire des Echanges Membranaires et Signalisation, UMR 6191 CNRS/CEA/Université Aix-Marseille II, DEVM/CEA Cadarache, 13108 S<sup>t</sup> Paul les Durance Cedex, France. <sup>c</sup> Institut de Biologie Physico-Chimique, UMR 7141 CNRS/Université Paris 6, 13 rue P. et M. Curie, 75005 Paris, France. <sup>d</sup> Laboratoire Canaux Ioniques, Fonctions et Pathologies, EMI 9931 CEA/INSERM/UJF, DRDC/CEA-Grenoble, 17 rue des Martyrs, 38054 Grenoble-cedex 9, France.

Running title: Role of HMA1 in chloroplast Cu homeostasis

Address correspondence to: Daphné Seigneurin-Berny and Norbert Rolland. Laboratoire de Physiologie Cellulaire Végétale, UMR 5168 CNRS/CEA/INRA/Université Joseph Fourier, DRDC/CEA-Grenoble, 17 rue des Martyrs, 38054 Grenoble-cedex 9, France. Tel. +33 4 3878 4986, Fax. +33 4 3878 5091. E-mail: [daphne.berny@cea.fr](mailto:daphne.berny@cea.fr), [nrolland@cea.fr](mailto:nrolland@cea.fr).

**Although ions play important roles in the cell and chloroplast metabolism, little is known about ion transport across the chloroplast envelope. Using a proteomic approach specifically targeted to the *Arabidopsis* chloroplast envelope, we have identified HMA1 which belongs to the metal transporting P<sub>1B</sub>-type ATPases family. HMA1 is mainly expressed in green tissues and we validated its chloroplast envelope localization. Yeast expression experiments demonstrated that HMA1 is involved in Cu homeostasis and that deletion of its N-terminal His-domain partially affects the metal transport. Characterization of *hma1 Arabidopsis* mutants revealed a lower chloroplast Cu content and a diminution of the total chloroplast SOD activity. No effect was observed on the plastocyanin content in these lines. The *hma1* insertional mutants grew like WT plants in standard condition but presented a photosensitivity phenotype under high light. Finally, direct biochemical ATPase assays performed on purified chloroplast envelope membranes showed that the ATPase activity of HMA1 is specifically stimulated by Cu. Our results demonstrate that HMA1 offers an additional way to the previously characterized chloroplast envelope Cu-ATPase PAA1 to import Cu in the chloroplast.**

Chloroplasts contain a large variety of ions among which metal ions such as Cu, Fe, Mn, Zn that are essential for their development and function. Cu is an essential redox cofactor required for a wide variety of processes, including photosynthetic electron transfer reactions (plastocyanin) and detoxification of superoxide

radicals (Cu/Zn superoxide dismutase, SOD)<sup>1</sup> (1). Other metal ions are cofactors for several enzymatic reactions: Zn is associated with chloroplast SOD, methionine synthase, carbonic anhydrase; Mn is required for oxygen evolution in photosynthesis whereas Fe is a cofactor of Fe SOD and is found in iron-sulfur clusters of cytochrome *b<sub>6</sub>f* complex, ferredoxin, photosystem I (PSI) and photosystem II (PS II) (2). All these metals are essential micronutrients but are toxic when present in excess (3). To maintain the concentration of metals within physiological limits, cells possess mechanisms that control the uptake, accumulation, trafficking and also detoxification of metal ions. Little is known about metal transport into chloroplasts. Until now, the sole chloroplast proteins demonstrated as being involved in metal ions transport are PAA1 (4) and very recently PAA2 (5), two P<sub>1B</sub>-type ATPases. PAA1, localized into the chloroplast envelope, supplies Cu to the chloroplast, whereas PAA2, localized into the thylakoid membrane, delivers Cu to the thylakoid lumen. One important information deriving from this work is the fact that the disruption of the *PAA1* gene does not fully abolish the import of Cu into the chloroplast. From this recent observation, Abdel-Ghany and coworkers (5) concluded that a yet unidentified and additional way to PAA1 must exist to import Cu into the chloroplast.

From proteomic analyses of *Arabidopsis* chloroplast envelope, we have identified several candidates for metal transport: putative ABC transporters (At1g70610, At2g01320, At5g58270, At5g03910, At4g25450), a magnesium transporter protein (At5g22830) and the P-type ATPase HMA1 (ref 6 and unpublished data).

P-ATPases are transmembrane proteins that couple ATP hydrolysis to the transport of various cations across membranes through a catalytic cycle involving the autophosphorylation of an Asp residue within a highly conserved DKTGT motif. P-ATPases are classified in several subgroups. Transition metal transporters are present within the P<sub>1B</sub>-ATPase subfamily (7). The vast majority of the characterized P<sub>1B</sub>-ATPases displays 8 predicted transmembrane helices with a typical CPC motif in the 6<sup>th</sup> helix that is essential for metal transport. They have been classified respectively in the P<sub>1B-1</sub> and P<sub>1B-2</sub> ATPases subgroup according to their specificity to either Cu<sup>+</sup>/Ag<sup>+</sup> or to Zn<sup>2+</sup>/Cd<sup>2+</sup>/Co<sup>2+</sup>/Pb<sup>2+</sup> (8). Such metal specificities are related to the presence of conserved residues, especially at the level of the 7<sup>th</sup> and 8<sup>th</sup> helix and can therefore be predicted from primary sequences. Among the 8 P<sub>1B</sub>-ATPases from *Arabidopsis* (for review see ref 9), *in silico* substrate predictions were experimentally confirmed for 6 transporters: PAA1, PAA2 and RAN1 (members of the P<sub>1B-1</sub> subgroup) and HMA2, HMA3 and HMA4 (members of the P<sub>1B-2</sub> subgroup). RAN1 was shown to be involved in the copper intracellular compartmentation allowing the supply of copper to ethylene receptors (10). Concerning HMA2-4, an increasing amount of data support the predictions that they are involved in zinc, cadmium and/or lead transport (11-15).

In contrast, the few experimental data on transporters of the P<sub>1B-4</sub> subgroup, such as HMA1 and OsHMA1, does not allow any accurate substrate and structure predictions. Since disruption of CoaT in *Synechocystis*, an enzyme of this group, reduces Co tolerance and increases Co accumulation (16), it was suggested that proteins of the P<sub>1B-4</sub> subgroup could be devoted to divalent cation transport, especially cobalt (8).

In this study, we report the identification and functional characterization of a new chloroplast P-type ATPase, HMA1. We first provide evidence for this protein to reside in the chloroplast envelope. We also demonstrate through yeast expression that HMA1 is involved in both zinc and copper homeostasis. Furthermore, characterization of *hma1 Arabidopsis* mutants reveals a decrease in chloroplast Cu content and in SOD activity and a photosensitivity phenotype under high light. Finally, measurements of ATPase activity in purified chloroplast envelope membranes demonstrates that HMA1 activity is specifically enhanced by Cu. Altogether these results demonstrate that HMA1 is an envelope ATPase involved in delivering copper ions to the stroma, where they are essential for the detoxification of active oxygen species formed during photosynthesis

under high light conditions.

## EXPERIMENTAL PROCEDURES

**Plant material and growth conditions** - *Arabidopsis* plants, Wassilevskija background (Ws), were germinated in Petri dishes containing solidified medium (Murashige and Skoog -MS-, 1% [w/v] sucrose, and 1% [w/v] agarose) for 2 weeks before transfer to soil. Plants were then grown in culture chambers at 23°C (12-h light cycle) with a light intensity of 150  $\mu\text{mol.m}^{-2}.\text{s}^{-1}$  in standard conditions. For phenotypic analyses, seeds were germinated in plates containing MS salts in absence or presence of CuSO<sub>4</sub> at various concentrations (0.1, 1, 10 and 50  $\mu\text{M}$ ), under different light intensities (50, 110, 280 and 340  $\mu\text{mol.m}^{-2}.\text{s}^{-1}$ ) for 4 weeks.

**Purification of chloroplast and chloroplast subfractions from *Arabidopsis*** - All operations were carried out at 0-5°C. Percoll-purified chloroplasts were obtained from 100-200 g of *Arabidopsis thaliana* leaves. Crude cell extracts and chloroplast subfractions were purified and stored as previously described (6). Analyses of the purity of chloroplast envelope preparations have shown a contamination with thylakoid protein between 1 and 3% (6). Chloroplasts purified for ICP-AES analyses were washed in the following resuspension buffer: 400 mM sorbitol, 20 mM Hepes/KOH pH 7.6, 2.5 mM EDTA, 5 mM MgCl<sub>2</sub>. Protein content was estimated using the BIO-RAD protein assay reagent (17). Chlorophyll content was determined by spectrophotometry in acetone solutions (18).

**Isolation of *HMA1* insertional mutants.** The *Arabidopsis hma1* mutants (lines ACT7 and DRC42) were identified by screening the FLAGdb/FST database (19) from the INRA (Versailles, France) collection of T-DNA insertional mutants. These lines, produced by *Agrobacterium*-mediated transformation (20), were transformed with a T-DNA construct (pGKB5 binary vector) that carries both *bar* and *nptII* selection markers. Primary transformants were self-pollinated to obtain plants homozygous for the insertion. To identify homozygous plants, PCR were carried out on genomic DNA using a primer for the T-DNA (Tag5: CTACAAATTGCCTTTTCTTATCGAC) and a gene specific primer (FST1: CACCTCGAAG ATCAGCCTCG for ACT7 line and FST2: AGTGAGCTCCTAATGTGCAGAGCTTAAACG for the DRC42 line). In addition, the two gene specific primers (FST1 and FST2) were used to detect plants that contain only a wt copy of the gene. The amplified bands were sequenced to confirm the T-DNA locations and orientations in *HMA1* gene. Segregation patterns were analyzed by

germinating progeny seeds on plates containing MS salts plus kanamycin (100 mg.l<sup>-1</sup>). Plants selected for further analysis segregated according to a 3:1 ratio, indicative of a single insert.

**Construction of vectors for stable expression in *Arabidopsis*** - To construct the vector for HMA1 overexpression in *Arabidopsis* Ws ecotype, the coding region of *HMA1* was PCR-amplified using the two flanking primers *BgIII-N*-ter (TCGAGATCTATGGAACCTGCAACTCTTACTC) and *SacI-C*-ter (AGTGAGCTCCTAATGTGCAGAGCTTAAACTG) from an *Arabidopsis* cDNA library. The PCR product was cloned into the pBluescript KS<sup>-</sup> vector (Stratagene). The *BgIII-SacI* fragment cleaved from this plasmid was inserted into the *BamHI-SacI* digested pEL103 binary vector (kanamycin resistance to transform wild-type plants). Plasmids used for *Agrobacterium tumefaciens* transformation were prepared using the "QIAfilter Plasmid Midi Kit" (Qiagen Laboratories; Germany).

***Arabidopsis* transformation** - Wild-type *Arabidopsis* plants (ecotype Ws) were transformed by dipping the floral buds of 4-weeks-old plants into an *Agrobacterium tumefaciens* (C58 strain) solution containing a surfactant (Silwett L-77) according to Clough and Bent (21). Primary transformants were selected on MS medium containing 100 mg.l<sup>-1</sup> kanamycin. Only lines segregating 3:1 for the resistance to kanamycin and expressing the recombinant protein were selected for further analysis. Primary transformants were then self-pollinated to obtain plants homozygous for the insertion.

**Construction of GFP reporter plasmids for transient expression in *Arabidopsis*** - The GFP reporter plasmid *Pro*<sub>35S</sub>:*sGFP(S65T)* and the plasmid containing the transit peptide (TP) sequence from RBCS fused to GFP [*Pro*<sub>35S</sub>:*TP-sGFP(S65T)*] were described previously (22). To express HMA1:GFP fusion, we PCR-amplified the entire sequence of *HMA1* using the primers *Sall-N*-ter (TTCGTCGACATGGAACCTGCAACTCTTACTCG) and *PciI-C*-ter (GCAACAGTTTAAGCTCTGCACATCACTGTGG) from an *A. thaliana* cDNA library. The PCR product was cloned into the pBluescript KS<sup>-</sup> vector (Stratagene). *Sall-PciI* fragment was inserted into the *Sall-NcoI* digested GFP reporter plasmid *Pro*<sub>35S</sub>:*sGFP(S65T)* to create the *Pro*<sub>35S</sub>:*HMA1-sGFP(S65T)* plasmid. From this construct, we extracted the entire cassette *Pro*<sub>35S</sub>-*HMA1-GFP-Nos* Ter using *EcoRI* and a partial *HindIII* digestion. This fragment was purified and inserted into the *EcoRI-HindIII* digested pEL103 binary vector (kanamycin resistance to transform wild-type plants). The plasmid used for *Agrobacterium tumefaciens* transformation were

prepared using the QIAfilter Plasmid Midi Kit (Qiagen Laboratories).

***Arabidopsis* leaves agroinfiltration** - Leaves from *Arabidopsis thaliana* (ecotype Ws) were injected with *Agrobacterium tumefaciens* strains harboring the appropriate plasmids according to (23). Three or four days after injection, localization of GFP and GFP fusions in leaves was analyzed by confocal fluorescence microscopy as previously described in (24).

**Foliar and chloroplastic metal content** - Leaves were dried for 48 h at 50°C. Chloroplasts and dried leaves were mineralized and metal content was determined using ICP-AES as previously described (25).

**RT-PCR** - *Arabidopsis thaliana* (Ws) plants were grown on sand up to 2 months with an 8 h photoperiod. Total RNA were extracted from various plant tissues with Trizol (Life Technologies). RT-PCR experiments were performed as previously described (25). We used the following primers to analyze the expression of *HMA1*, *PAA1* and *PAA2*: *HMA1* For (GATCATCACAACCACCATCATC) and *HMA1* Rev (CGCTTTTGTATGACAAATCAG); *PAA1* For (ACGGGTTATAGCAGGAG) and *PAA1* Rev (GTCGTTTCGGTTCGAG); *PAA2* For (AAAGGTGGTTTGGCCG) and *PAA2* Rev (GGACACTCCCATCGAC); *CSD2* For (TCCGT CGAAAGCGT TG) and *CSD2* Rev (GCCTCTGACTTAGAGCG).

**SDS-PAGE and western blot analyses** - SDS-PAGE analyses were performed as described by Chua (26). Proteins were revealed by coomassie-blue staining. For western blot analyses, gels were transferred to a nitrocellulose membrane (BA85, Schleicher and Schuell). The polypeptide corresponding to the predicted loop between amino acids 213 to 368 was produced in *E. coli* and purified for the production of a rabbit polyclonal antiserum. This antiserum was used, at a 1/1000 dilution, to detect HMA1. Plasma membrane and mitochondria were purified, from *Arabidopsis*, as previously described (27, 28). In order to validate purity of the membrane fractions, we used antibodies directed against envelope E37 (29), plasma membrane H<sup>+</sup>-ATPase (30), mitochondria TOM40 (31) and thylakoid LHCP (6).

**Superoxide dismutase activity** - SOD activity was performed according to McCord and Fridovich (32) with the following modifications. The reaction mixture consisted of 50 mM Hepes/KOH (pH 7.8) buffer, 0.5 mM EDTA, 4 mM xanthine, 0.5 mM nitroblue tetrazolium and 0.01 units of xanthine oxidase. A concentration curve was produced for each sample to calculate SOD activity. One unit of SOD activity was defined as the amount of extract that inhibited the rate of

nitroblue tetrazolium reduction by 50 %. The assays were carried out on purified stromal proteins.

**Cloning of HMA1** - A reverse transcription was performed on poly(A)<sup>+</sup> mRNA extracted from leaves of *Arabidopsis thaliana* (Ws ecotype). The open reading frame of *HMA1* was amplified by PCR using the primers 5'HMA1: CCATGGAACCTGCAACTCTTACTCGTTC and 3'HMA1: CCCCTAATGTGCAGAGCTTAAAC TGTTC, subcloned in the pCR<sup>®</sup>-XL-TOPO vector (Invitrogen<sup>™</sup>) and sequenced. This plasmid was modified to insert the *NotI* restriction site, allowing the subsequent cloning of the full length cDNA in the pYES2 yeast expression vector (Invitrogen<sup>™</sup>). Two truncated versions of *HMA1*, HMA1 $\Delta$ 60 and HMA1 $\Delta$ 89, deleted respectively from the first 60 and 89 amino acids were cloned in the pYES2-TOPO vector using respectively as forward primers HMA1 $\Delta$ 60for: CCGGAATTCC GGATGCTACGT GCTGTCGAAGATCACCATC and HMA1 $\Delta$ 89for: GGGATGGGATGCTGTTCTGTGGAATTGAAA GCGG. Both reactions were conducted using the reverse primer HMA1rev: AAGGAAAAAGCGG CCGAAAAGGAAAATAATGTGCAGAGCTT AAAGTGTG. Directed mutagenesis was performed on the pYES2-HMA1 $\Delta$ 60 plasmid using the Quickchange<sup>®</sup> kit (Stratagene), allowing the expression in yeast of D453A, S410C and H769E substituted versions of HMA1 $\Delta$ 60 or HMA1 $\Delta$ 89.

**Yeast expression, metal tolerance and accumulation** - BY4741 wild-type *Saccharomyces cerevisiae* strain (EUROSCARF acc. n<sup>o</sup>. Y00000) was transformed with the different plasmids and grown on synthetic medium as described in Gravot et al. (25), except that the precultures were performed with glucose 2% as carbon source to repress the protein expression. Drop-test experiments were performed using CuSO<sub>4</sub>, ZnSO<sub>4</sub>, NiCl<sub>2</sub> and CoSO<sub>4</sub> at various concentrations and growth was controlled from 2 to 5 days depending on the metal and the concentration. Liquid medium experiments were performed starting from a preculture with 2% [w/w] glucose, diluted in 30 ml to DO = 1 and then cultivated with 2% [w/w] galactose + 1% [w/w] raffinose for 24 h. Cells were then washed twice with 10 mM EDTA and twice with water. Yeast pellets were then dried at 50°C, mineralized and the metal content was analyzed using inductively coupled plasma-atomic emission spectrometer ICP-AES (Vista MPX, Varian).

**In vivo spectroscopic estimation of plastocyanin (PC)/photosystem I (PSI) ratios** - Estimation of the PC pool in WT and mutant chloroplasts was performed *in vivo* using an home built spectrophotometer, as previously described (33). Leaves were illuminated by a far red source at 720 nm in order to oxidize completely the PSI

donors' pool. Alternatively, experiments were performed in the presence of the PSII inhibitor 3-(3',4'-dichlorophenyl)-1,1-dimethylurea (DCMU). Absorption changes were detected by discrete flashes provided by a light-emitting-diode (LED) source that delivers 10  $\mu$ s square pulses. Light was filtered with appropriate filters, to select P<sub>700</sub> and PC redox changes. Absorption changes associated to P<sub>700</sub> redox changes were computed as  $\Delta I/I$  705 nm-  $\Delta I/I$  870 nm/2.  $\Delta I/I$  PC was computed as  $\Delta I/I$  870 nm +  $\Delta I/I$  705nm/10.

**ATPase assay** - ATPase activity was measured as the rate of ADP-dependent NADH oxidation in a coupled system containing NADH, phosphoenolpyruvate, pyruvate kinase and lactate dehydrogenase as described by Blumwald & Poole (34). The activity was monitored in the presence of Mg-ATP and after addition of 3 mM Cu, Co, Zn, Fe, Ag and Mn. The assays were performed on highly purified envelope proteins derived from chloroplasts of WT, *hma1* mutants and HMA1 overexpressing plants.

**Sequence analyses** - Subcellular localizations were predicted using the following programs: ChloroP at <http://www.cbs.dtu.dk/services/ChloroP/> (35) and Predotar at <http://genoplante-info.infobiogen.fr/predotar/> (36). The location of possible transmembrane helices was determined using the program ARAMEMNON at <http://aramemnon.botanik.uni-koeln.de/> (37). Sequence data from this article have been deposited with the GenBank data library under accession number AY907350 for *HMA1* (At4g37270).

## RESULTS

### HMA1 is localized in the chloroplast envelope

**Primary sequence analysis** - According to Argüello (8), and as predicted by hydropathy analysis (ARAMEMNON; ref 37), the membrane topology of HMA1 (At4g37270) suggests the presence of 6 or 7 transmembrane segments (TMs) with 4/5 in the *N*-half of the protein and two downstream of the large loop characterizing P-type ATPases (Fig. 1). HMA1 possesses the typical Ser-Pro-Cys motif in the 4<sup>th</sup>/5<sup>th</sup> TM rather than the usual Cys-Pro-Cys/His/Ser motif found in other P<sub>1B</sub>-ATPases. Furthermore, HMA1 has a His-rich region in its *N*-terminal part that could play a role in the function or regulation of this transporter since His residues often feature in metal-binding domains. The 6 TMs model would put both the His-rich region and the ATPase domain on the same side of the membrane, as for other P<sub>1B</sub>-ATPases (for review, see ref 9). These two domains would then

face the intermembrane space of the chloroplast envelope.

*In silico* analysis using ChloroP on HMA1 primary sequence (35) predicted the presence of a cleavable transit peptide (60 first amino acids; Fig. 1). However, other prediction programs (found in ARAMEMNON) predicted a mitochondrial localization. The experimental validation of the subcellular localization was therefore necessary.

*Validation of the subplastidial localization* - We first performed transient expression of HMA1-GFP fusion in *Arabidopsis* cells. Since the entire protein fused to GFP was not expressed in this system, we used the 119 first amino acids of HMA1 (including the predicted transit peptide) fused to GFP to transform *Arabidopsis* cells. Consistent with the prediction of ChloroP, HMA1-1/119 fused to GFP was associated to chloroplasts (Supplemental information 1). To validate the localization of the full-length protein, we also performed transient expression of HMA1-GFP fusion in *Arabidopsis* leaves. As expected (Fig. 2A), GFP alone was localized in the nucleus and the cytoplasm whereas the plastid control (the transit sequence of the small subunit of Rubisco fused to GFP) was targeted to the chloroplast. HMA1 fused to GFP was only detected in the chloroplasts from both epidermal and parenchymal cells, and no staining was observed in other membranes (Fig. 2A).

In order to strengthen this result, we then performed western blot experiments on purified subplastidial fractions, purified mitochondria and plasma membrane proteins. In good agreement with transient expression experiments, HMA1 was only detected in the envelope membranes (Fig. 2B) thus excluding the mitochondrial localization predicted in ARAMEMNON database (37). HMA1 was also not detected in two independent plasma membrane preparations thus excluding localization of HMA1 in this membrane system. Finally, the use of antibodies directed against markers from other membrane fractions, clearly demonstrates that association of HMA1 with the chloroplast envelope cannot be due to cross-contamination of envelope preparations with proteins from mitochondria, thylakoids or plasma membrane.

The expression of *HMA1* was analyzed by RT-PCR. *HMA1* transcripts were mainly detected in green tissues, which is consistent with a chloroplast localization of the protein (Fig. 2C). A comparative analysis was performed for the two other previously identified chloroplast Cu-ATPases. A faint expression was observed in roots thus suggesting a possible expression in non-green plastids. In good agreement with the work of Abdel-Ghany et al. (5), *PAA2* transcripts were detected in green tissues while *PAA1* transcripts were found in all analyzed

tissues (Fig. 2C) thus suggesting a broader role of *PAA1* in green and non-green plastids.

### **Functional characterization of HMA1 by expression in yeast**

*Heterologous expression of H1Δ60 impairs yeast cell growth and leads to cellular zinc and copper accumulation* - Heterologous expression of the complete *HMA1* cDNA was performed in *Saccharomyces cerevisiae* under the control of a galactose-induced promoter. We first observed that the yeast tolerance to Zn, Cu or Co was not altered in cells overexpressing HMA1 precursor and grown on metal-containing media (Fig. 3A). We also observed that the Zn and Co sensitivity of the hypersensitive yeast mutants *zrc1* and *cot1* was not modified by HMA1 overexpression (not shown). To determine whether the lack of phenotype of yeast mutants expressing the full-length HMA1 was due to lack of activity associated with the HMA1 precursor, we expressed in various yeast strains a truncated version of HMA1 (H1Δ60) in which the putative transit peptide (see Fig. 1) was deleted. The growth of H1Δ60-expressing cells was found to be strongly reduced after induction by galactose, even in the absence of excessive metal concentrations (Fig. 3B). To determine whether the protein toxicity was linked to its function, we designed a modified version of H1Δ60, in which the phosphorylated Asp453 from the DKTGT consensus sequence was replaced by an Ala. This substitution is known to prevent the P-ATPase catalytic turnover and impairs metal transport (38). Indeed, when expressed in yeast, the mutated H1Δ60-D453A protein was not toxic (Fig. 3B), suggesting that the toxicity of normal H1Δ60 protein could be due to its cation transport capacity. We also analyzed the growth in liquid medium of strains containing either the empty vector, the vector encoding H1Δ60, or the gene encoding the mutated H1Δ60-D453A protein. After an overnight induction with galactose, the OD of H1Δ60-expressing cells reached only 13% of the OD found in control cells or in H1Δ60-D453A-expressing cells. Higher levels of Cu and Zn were found in H1Δ60-expressing cells compared to control or H1Δ60-D453A-expressing cells (Table 1). As a whole, these results suggest that HMA1 is likely to regulate Cu and Zn homeostasis when expressed in yeast cells.

*HMA1 His-stretch deletion reverses the yeast growth impairment and reveals a Cu/Zn hypersensitivity* - In many P<sub>1B</sub>-ATPase, the *N*-ter soluble domain is involved in the regulation of metal transport. This is the case for the CxxC containing *N*-ter HMA domains from Cu<sup>+</sup>/Ag<sup>+</sup> ATPases of the P<sub>1B-1</sub> subgroup. His-rich *N*-ter domains of the CopB P<sub>1B-3</sub>-ATPase from the

archaeobacterium *Archeoglobus fulgidus* seems to regulate Cu<sup>2+</sup> transport in a similar way (39), since the deletion of the His-rich N-ter domain leads to a 40% reduction of the ATPase transport activity, without any modification of the affinity for the transported metal. To investigate the role of the 29 aminoacids His-rich stretch downstream the transit peptide (Fig. 1B), HMA1 deleted of the first 89 amino acids was expressed in yeast. This H1Δ89 version did not impair the cell growth on standard medium (Fig. 3C) suggesting that metal transport activity is affected by the deletion. This allowed testing the sensitivity of the expressing yeast to various metals. H1Δ89-expressing cells were found to be drastically hypersensitive to Zn and Cu (Fig. 3D) but not to Ni or Co (not shown). This phenomenon could reflect a residual metal transport activity of the H1Δ89 truncated protein, which could participate to cell intoxication at very high metal concentration. Indeed, those effects were reversed by the D453A substitution in the DKTGT motif, indicating that metal transport is involved in the observed phenotypes (Fig. 3D).

*S410C or H769D substitutions in H1Δ60 reverse the lethal phenotype and metal hypersensitivity* - Among the numerous specificities shared by the P<sub>1B-4</sub>-ATPases, are the conserved SPC motif, contrasting with the CP<sub>x</sub> consensus characteristic of others P<sub>1B</sub>-ATPases and the conserved HEG(G/S)T in the last predicted helix (8). Site-directed mutagenesis was performed on the pYES2-HMA1Δ60 plasmid to generate the S410C and H769D substitutions, located in the SPC and HEGG motifs from the 4<sup>th</sup>/5<sup>th</sup> and the last predicted helix respectively. We observed that both substitutions reversed the growth impairment phenotype conferred by H1Δ60 expression (Fig. 4). Moreover, neither H1Δ60-S410C nor H1Δ60-H769D expression induced Cu or Zn hypersensitivity in the transformed yeast cells. These results suggest that, in contrast with the Δ89 deletion, the S410C and H769D substitutions probably fully abolish metal transport capacities of HMA1. Those two residues are thus likely involved in the metal transduction process rather than in the transport rate regulation.

### **Functional characterization of HMA1 by *in planta* analysis**

*Identification of homozygous insertional hma1 mutants and production of HMA1 overexpressing plants* - Two T-DNA insertion lines in the HMA1 gene, lines ACT7 and DRC42 from the FLAGdb/FST database (INRA Versailles, France) were identified. In both lines, the T-DNA is inserted in the 11<sup>th</sup> intron in the same region but in opposite orientations (Fig. 5A and Supplemental information 2). We isolated homozygous insertion

mutants by segregation analysis on kanamycin and by PCR with specific primers of the HMA1 gene and with a T-DNA reverse primer (Tag5, corresponding to the 5' part of the T-DNA; see Fig. 5A). Two homozygous mutants were obtained for each insertion line by self-cross, named ACT7 #1, ACT7 #23, DRC42 #4 and DRC42 #12. To analyze the impact of the insertions in these lines, HMA1 transcripts analyses were performed with various primers in front and behind the T-DNA insertion. In good agreement with the localization of the insertion (Fig. 5A), these experiments resulted in the amplification of the 5' part of HMA1 mRNA but no amplification of the 3' part of HMA1 could be detected (see Fig. 5B). To validate the absence of the HMA1 protein in these lines, subplastidial fractions were prepared from these mutant plants. As shown in Fig. 5C, HMA1 was detected in the envelope from WT chloroplasts but not in the envelope from chloroplasts of *hma1* mutants (lines ACT7 and DRC42).

Six stable transformed plants expressing HMA1 under the control of the constitutive 35S promoter were also obtained (see Methods). For each of these transformants, the amount of HMA1 was determined by western blot on crude membrane protein extracts. As shown in Fig. 6A, HMA1 was detected at a low amount in WT extract, undetected in the extracts from T-DNA insertion lines, and overexpressed in stable transformant plants 1, 2 and 6. We then analyzed by western-blot whether the overexpressed HMA1 was present in envelope membranes. Indeed, it was detected, like the native protein, only in the chloroplast envelope fraction where it was much more abundant (10-20 times) when compared to the native protein detected in WT plants (Fig. 6B).

*Metal ion content in WT, insertional and overexpressing mutants* - When grown in standard conditions, *hma1* and overexpressing mutants did not show any apparent morphological phenotype when compared to WT plants. As HMA1 is involved in metal transport, we analyzed by ICP the transition metal ions content of these different lines. Leaves and purified chloroplasts were obtained from plants grown in soil in standard conditions. No significant difference was found, in the leaves of these plants, for the content of the various ions analyzed and notably for Cu and Zn (Fig. 7C). Chloroplast Cu levels were comparable in WT and overexpressing plants. However, in chloroplasts from *hma1* mutant lines, Cu content was halved with respect to chloroplasts from WT or overexpressing plants (Fig. 7A). No difference was observed for the content of chloroplast Zn (Fig. 7B), Co or for any other ions analyzed (not shown).

*Phenotypic analysis of hma1 mutants and*

*overexpressing plants* - Overexpressing and insertional mutant plants did not display any obvious phenotype under standard condition although *hmal* mutants showed a decreased Cu content. However, Cu is an important cofactor for chloroplast proteins like plastocyanin or SOD (1). We thus tested the impact of Cu and of an excess of light on the growth of these different lines. In all conditions tested, the overexpressing plants did not show any visible difference with the WT plants. Under low light intensities (50 and 110  $\mu\text{mol}\cdot\text{m}^{-2}\cdot\text{s}^{-1}$ , Fig. 8) and for all Cu concentrations tested (not shown), we found that *hmal* mutant plants grew like WT plants. In contrast, under high light (above 280  $\mu\text{mol}\cdot\text{m}^{-2}\cdot\text{s}^{-1}$ ), *hmal* mutants exhibited a strong photosensitivity phenotype leading to white leaves with restricted green regions. Some mutant plants were dwarf and totally white, others had several white leaves with some green regions and a few showed little differences with WT plants. This phenotype was fully reproducible and observed in absence of Cu and at various Cu concentrations in the media (0.1, 1 and 10  $\mu\text{M}$ ). In the presence of 50  $\mu\text{M}$  Cu the growth of all plants was affected by the toxic Cu concentration and so, differences between WT and *hmal* mutants were less evident. We also noted that this phenotype seems to depend on a threshold since all the seedlings do not respond similarly and since the leaves show a variegated phenotype. This phenotype demonstrates that HMA1 is necessary to allow plant growth under high light, probably through its role in delivering Cu to chloroplast proteins or enzymes highly active in such growth condition.

*SOD activity and plastocyanin content* - Cu is a cofactor for Cu/Zn SOD and plastocyanin. We therefore analyzed the SOD activity and the plastocyanin content in chloroplasts of mutants and overexpressing plants. The total SOD activity was measured in stromal proteins purified from all plants. We observed an important diminution of the total SOD activity in the stroma of *hmal* mutant (Fig. 9B) while no significant difference was observed between stromal SOD activity from WT and overexpressing plants. It is interesting to note that the *CSD2* (the chloroplast Cu/Zn SOD) transcripts showed a reduced expression in *hmal* mutant leaves (see Fig. 9A) when compared to expression levels detected in leaves from WT and overexpressing plants. This is in good agreement with the results of Abdel-Ghany and co-workers (5) who showed that the decrease of Cu in the stroma leads to a decrease of the *CSD2* activity (resulting from the lack of Cu) but also to a decrease of the *CSD2* transcripts. They have suggested that Cu is sensed in the stroma of the chloroplast and that this signal influences transcripts level of the chloroplast

Cu/Zn SOD (5).

We then analyzed the plastocyanin content of mutant and WT chloroplasts by spectroscopic analysis *in vivo*. In contrast to SOD, the plastocyanin levels were not affected in the lumen of *hmal* mutant chloroplasts (Table 2). This suggests that either the affinity of the plastocyanin for Cu is enough to compensate for a decrease in Cu chloroplast concentration induced by the mutation, or that the affinity of the thylakoidal Cu-transport machinery is large enough to maintain Cu homeostasis in the thylakoid lumen.

*ATPase assay on chloroplast envelope* - In order to have a direct biochemical evidence for the ATPase activity and specificity of the HMA1 protein, we choose to measure its activity on chloroplast envelope membranes purified from the different plants available. This assay was performed to determine (a) whether the expression level of HMA1 could modify the ATPase activity of the chloroplast envelope and (b) whether this activity was modified by the presence of ions. This assay allows the measurement of total envelope ATPase activities among which PAA1, HMA1 ( $P_{1B}$ -type ATPases which may be sensitive to addition of metal ions) and also other unidentified ATPases.

As shown in Table 3, the ATPase activity associated to chloroplast envelope membranes is reduced in *hmal* mutants (*hmal* KO) due to the lack of HMA1 activity. On the contrary, this ATPase activity is enhanced in envelope membranes from plants overexpressing the HMA1 protein (Ox 1, 2 and 6; see Fig. 6). This first observation is in good agreement with an ATPase activity associated to the HMA1 protein.

It is important to note that ATPase activities of very similar values were measured in the presence of  $\text{Co}^{2+}$  or  $\text{Zn}^{2+}$  ions (Table 3) suggesting that these ions have no impact on the HMA1 activity (but also on any other chloroplast envelope associated ATPases). Similarly, addition of  $\text{Ag}^{2+}$ ,  $\text{Mn}^{2+}$  or  $\text{Fe}^{2+}$  did not affect the ATPase activity measured in the envelope from the various plants (not shown). However, when the assay was performed in the presence of Cu, a significant increase of the ATPase activity was detected, especially in the envelope from HMA1 overexpressing plants (Ox; see Table 3). This second observation clearly demonstrates that HMA1 activity is specifically stimulated by Cu. The increase of the total ATPase activity observed in the envelope from the *hmal* insertion mutants and in the presence of Cu is most probably due to the activation of the PAA1 protein since this ATPase was also demonstrated to be associated to the chloroplast envelope and involved in Cu homeostasis (see ref 5). This experiment then

provides the first direct biochemical evidence for a Cu-stimulated ATPase activity associated to both HMA1 and PAA1. The increase of total ATPase activity observed in envelope from WT plants then most probably accounts for the stimulation of both HMA1 and PAA1.

In order to have an estimation of the respective activities of HMA1 and PAA1 (and other yet uncharacterized chloroplast envelope ATPases), we compared the ATPase activities measured in the envelope from WT, *hma1* mutants and overexpressing plants. This provides an estimate of (a) the specific activity of HMA1 and (b) the PAA1 and other ATPase activity. Indeed, the activity measured in the envelope from *hma1* mutants corresponds to the PAA1 activity and other unidentified ATPases of the chloroplast envelope. Thus, subtraction of the total activity measured in WT or overexpressing plant to the activity measured in the *hma1* mutant gives an estimation of the specific activity of HMA1 in these plants (see Table 3).

On this basis, one can note that the HMA1 activity is increased about 12 times in overexpressing plant and in the presence of Cu (Table 3), which is in good agreement with the level of accumulation of overexpressed HMA1 protein in envelope membrane from these plants (see Fig. 6).

Finally, and in good agreement with these direct biochemical observations, we could demonstrate that deletion or overexpression of HMA1 has no impact on the expression of both PAA1 and PAA2 (supplemental information 3). Both biochemical analysis and expression studies (Table 3 and supplemental information 3) thus demonstrate that PAA1 can not compensate for the lack of HMA1.

## DISCUSSION

**HMA1 is a P<sub>1B</sub>-ATPase of the chloroplast envelope** - Proteomic analyses of chloroplast envelope membranes (Refs 6, 40 and unpublished results) led to the identification of hundreds of proteins, among which we found HMA1 that belongs to the P<sub>1B</sub>-ATPases, a subgroup of the P-type ATPases involved in metal ions transport (3). We demonstrated its chloroplast envelope localization using both transient expression in *Arabidopsis* leaves and cultured cells, and western blot analyses performed on subplastidial fractions (Fig. 2). HMA1 is therefore the second P<sub>1B</sub>-ATPase identified in the chloroplast envelope, the first one being the ATPase PAA1 (5). The presence of such transporters was expected since metals play a key role in chloroplast metabolism. HMA1 belongs to the P<sub>1B-4</sub>-ATPases which display only 6 (8) or 7

(ARAMEMNON) predicted helix instead of 8 and share a specific SPC motif instead of the classical CPx consensus. HMA1 lacks the *N*-ter *Heavy Metal Associated* regulatory domain usually found in P<sub>1B</sub>-ATPases. Instead, it has a long His stretch reminding the *N*-ter domain of the P<sub>1B-2</sub> Bxa1 from *Oscillatoria brevis* that was described as transporting both copper and zinc (41).

It is worthy to note that the orthologue OsHMA1 in rice shares the same structural properties (42) and is predicted to be chloroplast located by Predotar (36). Moreover the green alga *Chlamydomonas reinhardtii* displays two putative organelle-targeted P<sub>1B</sub>-ATPases, namely CrHMA1 and CrHMA3, that are respectively orthologues of HMA1 and PAA1/PAA2 (43), suggesting that the presence of two subgroups of copper transporting P<sub>1B</sub>-ATPases is necessary even in this phylogenetically distant photosynthetic eukaryote. In *Cyanidioschyzon merolae*, a unicellular red alga considered to belong to the most primitive eukaryotic phylum (44), CmHMA1 is even the only putative organelle-targeted P<sub>1B</sub>-ATPase (43). This suggests an essential role for this transporter in supplying Cu to the single chloroplast of this organism.

**HMA1 expression in yeast affects Cu and Zn homeostasis** - Yeast heterologous expression is an efficient tool that allowed the functional characterization of many plant metal transporters. The fact that yeast cells expressing H1Δ60 contain more Cu and Zn than wild type cells reflects an impairment of the homeostasis for those two metals. A possibility would be that H1Δ60 is addressed to the yeast plasma membrane, importing Cu and Zn from the medium into the cytoplasm. The major drawback of this hypothesis is that P<sub>1B</sub>-ATPases are generally considered to transport metals from the cytoplasmic side of membranes to the other side (8). A more likely hypothesis is that H1Δ60 is addressed to yeast internal membranes, loading Cu and Zn from the cytoplasm into a metal-sensitive compartment. The resulting cytoplasmic metal depletion could trigger an enhancement of metal import processes, accounting for the higher Cu and Zn content in H1Δ60-expressing cells.

As H1Δ60-expressing cells grow at a very low rate, we were unable to test whether added metals could accentuate the lethal phenotype to validate that metal homeostasis impairment is the actual cause of the growth stop. In H1Δ89-expressing cells, a residual transport activity offers the possibility to explore metal specificity of HMA1. The fact that such yeast cells were still highly sensitive to Cu and Zn suggest that both metals can be transported by HMA1 in yeast. However, due to the Cu specificity of HMA1

observed *in planta* (low Cu content in the chloroplasts from *hmal* knock-out lines and Cu-specific stimulation of HMA1 activity, see latter) we can not exclude that the impact of HMA1 expression on Zn concentrations measured in yeast cells results from an indirect effect.

Proteins from the P<sub>1B-4</sub>-subgroup display strong originality at the structural level, the first being the number of predicted helices, which is probably lower than the 8 helices found in P<sub>1B-1</sub> and P<sub>1B-2</sub>-ATPases. Both OsHMA1 and HMA1 display a His-rich motif at the *N*-ter part of the protein. Yeast expression experiments (Fig. 3) led to the conclusion that this stretch could play a role in metal transport regulation. This is consistent with experiments performed on His-rich domains in other P<sub>1B-3</sub>-ATPases (39) and P<sub>1B-2</sub>-ATPases (15).

The CPx motif in the 6<sup>th</sup> predicted helix is widely accepted as a component of a metal translocation/binding site. However, a recent study with CopA from *Archaeoglobus fulgidus* demonstrated that other residues from the 7<sup>th</sup> and the 8<sup>th</sup> helices are required for Cu<sup>+</sup> coordination during transport (45). The present study strongly suggests that the Ser residue from the SPC motif in HMA1 is essential for metal transport and that it can not be substituted by a Cys. We also showed that the His residue from the HEGG motif in the last helix probably plays a role in transport. This confirms the alignment-based predictions of Argüello (8), and highlights the specificity of the Ser residue in P<sub>1B-4</sub>-ATPases.

**Disruption of HMA1 affects Cu content in chloroplasts and leads to photosensitivity under high light conditions** - Whereas the metal content in leaves from the different genotypes was comparable, the Cu content in *hmal* mutant chloroplasts was only half the one in WT plants (Fig. 7). This result points out the importance of analyzing purified chloroplasts as the Cu deficiency was undetectable at the organ level. Altogether, the data from yeast expression and the low Cu content in *hmal* chloroplasts suggest that HMA1 is involved in Cu uptake into chloroplasts. The specificity of HMA1 for Cu was also confirmed by direct biochemical evidences, since ATPase assays performed on chloroplast envelope demonstrated that HMA1 ATPase activity was exclusively stimulated by Cu and not by Zn, Co, Fe, Mn or Ag. As the specificity of the protein deduced from its expression in heterologous system is slightly different to the one identified in its native context, this underlined the importance of the characterization *in planta*. This specificity for Cu is in perfect correlation with the reduced content of Cu ions measured in chloroplasts from *hmal* plants.

The resulting Cu content in *hmal* chloroplasts is likely to result from PAA1 activity (5) or other still unidentified Cu transporters.

In chloroplasts, Cu is a cofactor for plastocyanin which transfers electrons from cytochrome *b<sub>6</sub>f* to PSI and for the chloroplast Cu/Zn SOD that is a critical component of the active-oxygen-scavenging system (46). Thus, we analyzed the impact of Cu and high light on the growth of the mutant lines. High concentration of Cu (50  $\mu$ M) led to the inhibition of leaf expansion and destruction of chlorophylls. This toxicity appeared for all the plants analyzed (data not shown) probably due to a toxic cytoplasm Cu concentration. Surprisingly, there was no phenotypic variation between WT, overexpressing and insertional plants for all Cu concentrations used. No enhanced sensitivity of overexpressing plants to Cu was observed which is consistent with the WT levels of Cu found in the chloroplasts from overexpressing plants. This suggests a tight regulation of the cell Cu uptake and also the presence of a Cu regulation system in the chloroplast such as saturation of metallochaperone or presence of protein involved in Cu efflux.

Under high light, the *hmal* lines present a photobleaching that is not observed in WT and overexpressing plants (Fig. 8). This photosensitivity was not rescued by addition of Cu in the medium. Such a phenotype is consistent with the diminution of the Cu content in chloroplasts from *hmal* mutants. Cu/Zn SODs are ubiquitous metalloenzymes that catalyze the reduction of superoxide (O<sub>2</sub><sup>-</sup>) to hydrogen peroxide and molecular oxygen (32), a reaction that constitutes the first cellular defense against many oxidative stress situations (47). Reactive oxygen species, like O<sub>2</sub><sup>-</sup>, are mainly formed in the chloroplast where light harvesting and electron transport lead to the formation of singlet oxygen and superoxide anion radicals (48). In this study, in *hmal* mutant grown in normal conditions, we found a reduction of the total chloroplast SOD activity but no variation of the plastocyanin content (Fig. 9, table 2). The diminution of SOD activities could account for the photosensitivity phenotype. Different pathways are thought to cooperate to respond to photooxidative stress: the zeaxanthin cycle, the cyclic electron flow and the water-water cycle that involve SOD and ascorbate peroxidase enzymes (49). Characterization of chloroplast Cu/Zn SOD knockdown and overexpressing plants suggest that this SOD plays an essential role in photooxidative stress (46, 49).

We can hypothesize that under low light intensity, the remaining level of Cu in chloroplasts from *hmal* mutant plants is sufficient to supply the needs for the active plastocyanin and part of the

chloroplast SOD. In these conditions, the remaining SOD activity is sufficient to scavenge the low amount of reactive oxygen species that are produced. However, under higher light intensity, the release of reactive oxygen species is enhanced and SODs have to respond to this oxidative stress. In this case, chloroplast SOD activities in the *hma1* mutant are probably insufficient to reduce the pool of reactive intermediates produced, causing destruction of chlorophylls and in turn, inhibition of photosynthesis. This observation also suggests that other photoprotection systems are not able to compensate for the decrease of SOD activity.

**Which function for HMA1 in the chloroplast?** - HMA1 and PAA1 are two  $P_{1B}$ -type ATPases involved in the transport of Cu into chloroplasts but the disruption of the corresponding genes have different consequences. *hma1* mutants contain less chloroplast Cu and SOD activity without any detectable impact on plastocyanin and pigment contents. *hma1* mutants also display a photosensitivity phenotype under high light, that is not reversed by addition of Cu in the media. In *paal* mutants (4), Cu content is also halved, but the pool of plastocyanin is severely affected and the activity of Cu/Zn SOD, electron transport and chlorophyll content are diminished. Furthermore, Cu addition rescues the *paal* phenotype. Altogether, these results suggest that these two  $P_{1B}$ -ATPases play different roles in the regulation of Cu homeostasis and transport.

From our observations and the data from Abdel-Ghany et al. (5), we can conclude that the *Arabidopsis hma1* and *paal* mutants have a different behavior upon addition of Cu to the culture medium. *paal* mutants recover a WT phenotype (5) probably owing to the action of the HMA1 protein and its capacity to import Cu. In contrast, in *hma1* mutants, the phenotype observed is not reversed by addition of Cu, thus PAA1 seems to function at its maximum rate and is probably not able to provide more Cu to the chloroplast. This hypothesis is reinforced by ATPase measurements (Table 3) which showed, in *hma1* mutant and in the presence of high concentration of Cu (3 mM), that PAA1 is unable to compensate for the lack of HMA1 activity.

$P_{1B}$ -ATPases are generally specific to either monovalent or divalent cations. Since Cu can be found both as a monovalent or divalent ion, the apparent redundancy between HMA1 and the recently described  $P_{1B-1}$ -ATPase PAA1 at the chloroplast envelope could hide their specific role in the transport of divalent and monovalent Cu. Further biochemical work is needed to ascertain this hypothesis.

It has been proposed that PAA1 provides Cu to a metallochaperone that could interact with the chloroplast Cu/Zn SOD and also to PAA2, a  $P_{1B}$ -ATPase localized in the thylakoids (5). Then, PAA1 could be the major Cu transport system into chloroplasts to supply Cu for photosynthesis. This hypothesis is strengthened by our measurements of ATPase activities in purified envelope membranes from overexpressing plants. These assays show that HMA1 activity represents about one third of the total activity (see Table 3) in the various conditions analyzed. As it seems unlikely that other Cu-ATPases are present in the chloroplast envelope, the increase of activity observed in the presence of Cu is most likely due to HMA1 and PAA1 activities. Thus, by comparing the results obtained in control condition and in the presence of Cu for WT and *hma1* mutant lines (Table 3), we estimated that HMA1 activity increases 1.5 times (from 37% to 56% with Cu) and PAA1 activity at least 3.2 times (from 63% to 204% with Cu, and considering that the 63% can account for other ATPase activity). On a quantitative point of view, the activity of HMA1 seems thus to be lower than that of PAA1 in the chloroplast envelope. However it should be kept in mind that despite its lesser ATPase activity levels, HMA1 physiological function seems to be irreplaceable in light-stressing conditions as *PAA1* gene expression and PAA1 protein activity can not compensate for the lack of HMA1.

While more expressed in leaves when compared to non-green tissues, PAA1 is relatively abundant in all tested plant tissues (Fig. 2C). On the contrary, HMA1 is mainly expressed in green tissues suggesting that it is important for an optimal functioning of chloroplasts. Interestingly, HMA1 and PAA2 present very similar expression profiles (Fig. 2C) thus suggesting that the role of both enzymes is more important in chloroplasts where larger amounts of Cu might be required for photosynthesis (PAA2) and to respond to oxidative stress (HMA1). A weak expression of HMA1 was also detected in roots. This might be related to the fact that a Cu/Zn SOD seems to be present in plastids of roots (50, 51) and that oxidative stresses also occur in roots. We thus can not exclude a role for HMA1 in non-green plastids.

Finally, our work suggests that plastids need different Cu transport systems and a tight regulation of these Cu delivering pathways to supply photosynthesis and to respond to oxidative stress generated in high light conditions. PAA1 and HMA1 are not just redundant proteins in term of physiological function. Then, more than identifying an alternative import pathway for Cu, we provide evidence for an alternative role of HMA1, which is

its specific requirement for the plant to grow under adverse light conditions.

## REFERENCES

1. Fox, T.C. and Guerinot, M.L. (1998) *Plant Mol. Biol.* **49**, 669-696
2. Raven, J.A., Evans, M.C.W., and Korb, R.E. (1999) *Photosynth. Res.* **60**, 111-149
3. Williams, L.E., Pittman, J.K., and Hall, J.L. (2000) *Biochim. Biophys. Acta* **1465**, 104-126
4. Shikanai, T., Müller-Moulé, P., Munekage, Y., Niyogi, K.K., and Pilon, M. (2003) *Plant Cell* **15**, 1333-1346
5. Abdel-Ghany, S.E., Müller-Moulé, P., Niyogi, K.K., Pilon, M., and Shikanai, T. (2005) *Plant Cell* **17**, 1-19
6. Ferro, M., Salvi, D., Brugiere, S., Miras, S., Kowalski, S., Louwagie, M., Garin, J., Joyard, J., and Rolland, N. (2003) *Mol. Cell. Proteomics* **2**, 325-345
7. Palmgren, M.G. and Axelsen, K.B. (1998) *Biochim. Biophys. Acta* **1365**, 37-45
8. Argüello, J.M. (2003) *J. Membr. Biol.* **195**, 93-108
9. Williams, L.E. and Mills, R.F. (2005) *Trends in plant sci.* **10**, 491-502
10. Hirayama, T., Kieber, J.J., Hirayama, N., Kogan, M., Guzman, P., Nourizadeh, S., Alonso, J.M., Dailey, W.P., Dancis, A., and Ecker, J.R. (1999) *Cell* **97**, 383-393
11. Mills, R.F., Krijger, G.C., Baccarini, P.J., Hall, J.L., and Williams, L.E. (2003) *Plant J.* **35**, 164-176
12. Mills, R.F., Francini, A., Ferreira da Rocha, P.S., Baccarini, P.J., Aylett, M., Krijger, G.C., and Williams, L.E. (2005) *FEBS Lett.* **579**, 783-791
13. Hussain, D., Haydon, M.J., Wang, Y., Wong, E., Sherson, S.M., Young, J., Camakaris, J., Harper, J.F., and Cobbett, C.S. (2004) *Plant Cell* **16**, 1327-1339
14. Verret, F., Gravot, A., Auroy, P., Leonhardt, N., David, P., Nussaume, L., Vavasseur, A., and Richaud, P. (2004) *FEBS Lett.* **576**, 306-312
15. Verret, F., Gravot, A., Auroy, P., Preveral, S., Forestier, C., Vavasseur, A., and Richaud, P. (2005) *FEBS Lett.* **579**, 1515-1522
16. Rutherford, J.C., Cavet, J.S., and Robinson, N.J. (1999) *J. Biol. Chem.* **274**, 25827-25832
17. Bradford, M. (1976) *Anal. Biochem.* **72**, 248-254
18. Bruinsma, J. (1961) *Biochim. Biophys. Acta* **52**, 576-578
19. Samson, F., Brunaud, V., Balzergue, S., Dubreucq, B., Lepiniec, L., Pelletier, G., Caboche, M., and Lechamy, A. (2002) *Nucleic. Acids Res.* **30**, 94-97
20. Bechtold, N., Ellis, J., and Pelletier, G. (1993) *CR Acad. Sci. Paris Life Sci.* **316**, 1194-1199
21. Clough, S.J. and Bent, A.F. (1998) *Plant J.* **16**, 735-743
22. Chiu, W., Niwa, Y., Zeng, W., Hirano, T., Kobayashi, H., and Sheen, J. (1996) *Curr. Biol.* **6**, 325-330
23. Lavy, M., Bracha-Drori, K., Sternberg, H., and Yalovsky, S.A. (2002) Cell-specific, prenylation-independent mechanism regulates targeting of type II RACs. *Plant Cell* **14**, 2431-2450
24. Miras, S., Salvi, D., Ferro, M., Grunwald, D., Garin, J., Joyard, J., and Rolland, N. (2002) *J. Biol. Chem.* **277**, 47770-47778
25. Gravot, A., Lieutaud, A., Verret, F., Auroy, P., Vavasseur, A., and Richaud, P. (2004) *FEBS Lett.* **561**, 22-28
26. Chua, N.H. (1980) *Methods Enzymol.* **69**, 434-436
27. Marmagne, A., Rouet, M.A., Ferro, M., Rolland, N., Alcon, C., Joyard, J., Garin, J., Barbier-Brygoo, H., and Ephritikhine, G. (2004) *Mol. Cell. Proteomics* **3**, 675-691
28. Brugiere, S., Kowalski, S., Ferro, M., Seigneurin-Berny, D., Miras, S., Salvi, D., Ravel, S., d'Herin, P., Garin, J., Bourguignon, J., Joyard, J., and Rolland, N. (2004) *Phytochemistry* **65**, 1693-707
29. Teyssier, E., Block, M.A., Douce, R., and Joyard, J. (1996) *Plant J.* **10**, 903-12.
30. Morsomme, P., Dambly, S., Maudoux, O., and Boutry, M. (1998) *J. Biol. Chem.* **273**, 34837-34842
31. Werhahn, W., Niemeyer, A., Jansch, L., Kruff, V., Schmitz, U.K., and Braun, H. (2001) *Plant Physiol.* **125**, 943-954
32. McCord, J.M. and Fridovich, I. (1969) *J. Biol. Chem.* **244**, 6049-6055
33. Joliot, P. and Joliot, A. (2005) *Proc. Natl. Acad. Sci. U S A* **102**, 4913-4918
34. Blumwald, E., and Poole, R.J. (1985) *Proc. Natl. Acad. Sci. USA* **82**, 3683-3687
35. Emanuelsson, O., Nielsen, H., and von Heijne, G. (1999) *Protein Sci.* **8**, 978-984
36. Small, I., Peeters, N., Legeai, F., and Lurin, C. (2004) *Proteomics* **4**, 1581-1590

37. Schwacke, R., Schneider, A., Van Der Graaff, E., Fischer, K., Catoni, E., Desimone, M., Frommer, W.B., Flüge, U.I., and Kunze, R. (2003) *Plant Physiol.* **131**, 16-26
38. Møller, J.V., Juul, B., and le Maire, M. (1996) *Biochim. Biophys. Acta* **1286**, 1-51
39. Mana-Capelli, S., Mandal, A.K., and Argüello, J.M. (2003) *J. Biol. Chem.* **278**, 40534-40541
40. Ferro, M., Salvi, D., Rivière-Rolland, H., Verdat, T., Seigneurin-Berny, D., Garin, J., Joyard, J., and Rolland, N. (2002) *Proc. Natl. Acad. Sci. USA* **99**, 11487-11492
41. Tong, L., Nakashima, S., Shibasaka, M., Katsuhara, M., and Kasamo, K. (2002) *J. Bacteriol.* **184**, 5027-5035
42. Baxter, I., Tchieu, J., Sussman, M.R., Boutry, M., Palmgren, M.G., Gribskov, M., Harper, J.F., and Axelsen, K.B. (2003) *Plant Physiol.* **132**, 618-628
43. Hanikenne, M., Krämer, U., Demoulin, V., and Baurain, D. (2005) *Plant Physiol.* **137**, 428-446
44. Matsuzaki, M., Misumi, O., Shin-I, T., Maruyama, S., Takahara, M., Miyagishima, S.Y., Mori, T., Nishida, K., Yagisawa, F., Nishida, K., Yoshida, Y., Nishimura, Y., Nakao, S., Kobayashi, T., Momoyama, Y., Higashiyama, T., Minoda, A., Sano, M., Nomoto, H., Oishi, K., Hayashi, H., Ohta, F., Nishizaka, S., Haga, S., Miura, S., Morishita, T., Kabeya, Y., Terasawa, K., Suzuki, Y., Ishii, Y., Asakawa, S., Takano, H., Ohta, N., Kuroiwa, H., Tanaka, K., Shimizu, N., Sugano, S., Sato, N., Nozaki, H., Ogasawara, N., Kohara, Y., and Kuroiwa, T. (2004) *Nature* **428**, 653-657
45. Mandal, A.K., Yang, Y., Kertesz, T.M., and Argüello, J.M. (2004) *J. Biol. Chem.* **279**, 54802-54807
46. Gupta, A.S., Webb, R.P., Holaday, A.S., and Allen, R.D. (1993) *Plant Physiol.* **103**, 1067-1073
47. Bowler, C., Van Camp, W., Van Montagu, M., and Inzé, D. (1994) *Crit. Rev. in Plant Sci.* **13**, 199-218
48. Levine, A. (1999) In *Plant responses to environmental stresses*, Lerner HR (ed) pp 247-264. New York: Marcel Dekker Inc
49. Rizhsky, L., Liang, H., and Mittler, R. (2003) *J. Biol. Chem.* **278**, 38921-38925
50. Kliebenstein, D.J., Monde, R.A. and Last, R.L. (1998) *Plant Physiol.* **118**, 637-650
51. Ruzsa, S.M., and Scandalios, J.G. (2003) *Biochemistry* **42**, 1508-1516

#### FOOTNOTES

\* D. S.-B. and A. G. contributed equally to this work.

<sup>1</sup>The abbreviations used are: Cu/Zn SOD, Cu/Zn superoxide dismutase; PS, photosystem; ICP-AES, Inductively coupled plasma-atomic emission spectrometry; TMs, transmembrane segments. GFP, green fluorescent protein.

We thank Marinus Pilon for sending proofs of his manuscript before publication. We also thank Ariane Atteia for critical reading of the manuscript, Geneviève Ephritikhine for the purified plasma membrane proteins and Solène Kowalski for the purified mitochondria. The TOM40, H<sup>+</sup>-ATPase and LHCP antibodies were obtained from Wolf Werhahn, Marc Boutry and Olivier Vallon respectively. Maryse Block is acknowledged for the gift of the E37 antibody. Thierry Lagrange is acknowledged for providing the pEL103 binary vector (originally constructed by Eric Lam).

This work was supported by CNRS and CEA (Toxicologie Nucléaire Environnementale) research programs.

#### FIGURE LEGENDS

**Fig. 1.** Structure of HMA1. (A) Primary sequence of HMA1. Predicted transit peptide (from ChloroP, ref 31) is indicated in italic. Transmembrane segments predicted by "ARAMEMNON" and according to Argüello (8) are underlined. Bold amino acids represent the conserved motifs among the P-type ATPase family. Grey boxes indicate the residues that could be involved in metal binding. The arrow indicates the position of the T-DNA insertion in mutant lines ACT7 and DRC42. (B) Schematic representation of the structure of HMA1 (adapted from ref 8): asterisk indicates the Asp residue which is phosphorylated during the catalytic cycle. Start codon location in the H1Δ60 and H1Δ89 versions are indicated by scissor symbols.

**Fig. 2.** HMA1 is localized in the chloroplast envelope. (A) Validation of the chloroplast localization by transient expression in *Arabidopsis* leaves. Transit peptide of the small unit of Rubisco fused to GFP (TP-GFP) was used as positive control. Localization of the GFP fusion proteins was analyzed in epidermal and parenchymal cells (B) Western blots on subplastidial fractions purified as previously described (devoid of any detectable non plastid contamination; see ref 6), plasma membrane and mitochondria. Proteins were

analyzed by coomassie blue-stained SDS-PAGE (upper part) and by western blot performed with a polyclonal antibody raised against HMA1 (lower part). Star indicates the position of HMA1. CE: crude extract, Chl: chloroplasts, E: envelope, S: stroma, T: thylakoids, PM: plasma membrane, M: mitochondria. Each fraction contained 15 µg proteins. Polyclonal antibodies raised against marker proteins were used to check cross-contaminations of purified fractions (E37 for plastid envelope, TOM40 for mitochondria, H<sup>+</sup>ATPase for plasma membrane, LHCP for thylakoids). (C) Expression of *HMA1*, *PAA1* and *PAA2* transcripts in different tissues. Expression profile was determined by RT-PCR on RNA extracted from various tissues. *ACTIN2* transcript was used as a control. L1m/L2m: one or two months old rosette leaves, R1m/R2m: one or two months old roots, St: stem, CL: cauline leaves, Fl: flowers.

**Fig. 3.** Functional characterization of HMA1 in the yeast system. Yeast cells with different plasmid (pYES2 as empty control plasmid) were grown as described in Methods and different dilutions were spotted on plates. (A) Yeast cells expressing the complete cDNA of HMA1 on galactose containing media supplemented with Cu, Zn or Co. (B) Yeast cells expressing HMA1, H1Δ60 and the H1Δ60-D453A substituted version, grown on media inducing (galactose) or repressing (glucose) heterologous protein expression. (C) Yeast cells expressing H1Δ60 and H1Δ89 on galactose containing medium. (D) Yeast cells expressing H1Δ89 and the H1Δ89-D453A substituted version on galactose containing media supplemented with Cu or Zn.

**Fig. 4.** Role of S410 and H769 residues of HMA1. Yeast cells expressing the cDNA of H1Δ60 and the substituted version H1Δ60-S410C and H1Δ60-H769D were grown on different media. (A) Glucose or galactose containing media respectively repressing and inducing the yeast heterologous expression. (B) Galactose containing media supplemented with Cu or Zn.

**Fig. 5.** Identification of homozygous *hma1* mutants. (A) PCR analyses. The genotype of the two independent insertion lines (ACT7 #1 and DRC42 #12) was analyzed by PCR using a primer for the T-DNA and a gene specific primer (T) or with two gene specific primers (G). Both insertions are localized within the 11<sup>th</sup> intron in opposite orientation. Hom: homozygous, Het: heterozygous, WT: wild type. Similar results were obtained with ACT7 #23 and DRC42 #4 lines (not shown). (B) Expression of *HMA1* in WT plants, *hma1* mutant (KO; ACT7 #23) and HMA1 overexpressing plants (Ox 2). Expression profile of *HMA1* transcripts was determined by RT-PCR on RNA extracted from leaves of the various plants. *ACTIN2* transcript was used as a control. Similar results were obtained with RNA extracted from DRC42 #12 and Ox 1 lines (not shown). (C) Validation of the absence of the HMA1 protein in *hma1* lines. Subplastidial fractions were purified from wild type (WT) and mutants (ACT7 #1 and DRC42 #12) plants as previously described (6). Each fraction contained 30 µg proteins. E: envelope, S: stroma, T: thylakoids. The amount of ACT7 #1 envelope proteins was twice important for the western blot. Proteins were analyzed by SDS-PAGE and revealed using coomassie blue staining, and western blot with a specific HMA1 antibody. The star indicates the expected position of HMA1.

**Fig. 6.** Identification of plants overexpressing HMA1. (A) Analysis of crude membrane protein extracts from the different genotypes. Membrane proteins were extracted from leaves of WT, KO and stable transformant plants (Ox). Each fraction contained 30 µg proteins. KO: insertion lines ACT7 #1 and DRC42 #12. Six stable transformant lines were obtained by *Agrobacterium* transformation and analyzed for the overexpression of HMA1. (B) Validation of overexpression of HMA1 in the chloroplast envelope. Subplastidial fractions were purified from wild-type (WT) and overexpressing plants (Ox 1 and 2). Each lane contained 15 µg proteins. E: envelope, S: stroma, T: thylakoids. In A and B, proteins were analyzed by coomassie blue-stained SDS-PAGE and western blot with an antibody raised against HMA1. The star indicates the position of HMA1.

**Fig. 7.** Cu and Zn contents in leaves and chloroplasts purified from WT, *hma1* insertional mutants and HMA1 overexpressing plants. Chloroplasts and leaves were mineralized and the metal content was determined by ICP measurements. Values are normalized according to the amount of Mg or chlorophyll of the chloroplasts analyzed and according to dry weight for leaves. The values are mean of results obtained from each insertion line (ACT7 #1, #23 and DRC42 #4, #12; KO) or overexpressing line (1, 2 and 6; Ox). WT: wild type. (A) Quantification of Cu content in purified chloroplasts. (B) Quantification of Zn content in purified chloroplasts. (C) Cu and Zn contents in leaves.

Fig. 8. Impact of high light on growth of *hma1* mutants. Seeds of the different lines were sown on plate containing MS salts and placed in different conditions of light intensity. Growth was monitored during four weeks. Insertion lines ACT7 #23 and DRC42 #4 represent one homozygous mutants obtained from the two independent insertion lines ACT7 and DRC42. Other homozygous plants (ACT7 #1 and DRC42 #12) deriving from the same insertion lines presented the same phenotype (not shown). Ox: overexpressing plants (Ox 1 and 2).

Fig. 9. SOD expression and activity. (A) Expression analysis of *CSD2* transcripts (the chloroplast Cu/Zn SOD) in leaves from WT, *hma1* mutants (KO; ACT7 #23) and HMA1 overexpressing plants (Ox 2). Expression profile of *CSD2* and *HMA1* transcripts was determined by RT-PCR on RNA extracted from leaves of the various plants. *ACTIN2* transcript was used as a control. 3' *HMA1*: amplification in the twelve and thirteenth exons, behind insertion of the T-DNA. (B) Measurement of the total SOD activity (Cu/Zn and Fe SODs) in purified chloroplasts from WT, *hma1* mutants and HMA1 overexpressing plants. SOD activity was measured spectrophotometrically on stromal proteins. WT: wild type; KO: mean value obtained for the four insertional lines (ACT7 #1, #23 and DRC42 #4, #12); Ox: mean value obtained for the three overexpressing line (Ox 1, 2 and 6).

TABLES

Table 1. Metal content in yeast grown on standard medium

	Zn	Cu	Mg
pYES	29.2 ± 3.3	2.24 ± 0.01	1860.6 ± 134.9
HMA1Δ60	186.3 ± 7.2	6.17 ± 0.45	2253.1 ± 68.6
H1Δ60-D453A	34.0 ± 6.9	2.57 ± 0.22	1923.6 ± 143.3

Metal content ( $\mu\text{g/g DW} \pm \text{SD}$ ) in yeast cells expressing the cDNA encoding H1Δ60 or its substituted version H1Δ60-D453A (control with the empty pYES2 plasmid) grown on galactose containing standard medium (metal content of the medium: Cu = 0.236  $\mu\text{M}$ ; Zn = 1.5  $\mu\text{M}$ ). Values presented represent the average of triplicate measurements  $\pm$  SD.

Table 2. Plastocyanin (PC)/photosystem I (PSI) stoichiometry in WT and mutants leaves.

Strain	WT	<i>hma1</i> mutants	Overexpressing plants
PC/PSI ratio	3 ± 0.40	2.9 ± 0.45	3.1 ± 0.38

Values refer to the size of the PC pool, normalized to the amount of P700<sup>+</sup>. They represent the average of quadruplicate measurements performed on WT and two independent mutant lines ACT7 #23, DRC42 #12 and Ox 1, Ox 2  $\pm$  SD. Similar results were obtained when the inhibitor DCMU was added to fully block photosystem II activity (not shown).

Table 3. HMA1 ATPase activity in envelope membranes is specifically enhanced by Cu. The total ATPase activity was measured in chloroplast envelope membranes purified from WT plants, the two independent *hma1* mutants (KO) and the three HMA1 overexpressing plants (Ox). WT: mean value  $\pm$  SD obtained for the two independent envelope preparations from WT plants. *hma1* KO: mean value  $\pm$  SD obtained for the two independent insertional lines (ACT7 #23 and DRC42 #12); Ox: mean value  $\pm$  SD obtained for the three independent HMA1 overexpressing lines (Ox 1, 2 and 6). The comparison of the activities obtained from the different genotypes gives access to an estimation of (a) the specific activity of HMA1 and (b) PAA1 and other potential ATPases activity (activity measured in *hma1* mutants). The sum of SD obtained for biochemical assays was added to estimated values of HMA1 activity (activity in WT or Ox lines minus activity in *hma1* mutant). 100% correspond to the value of ATPase activity measured in WT envelope in the presence of Mg-ATP, i.e. 0.46  $\pm$  0.003  $\mu\text{mol/h/mg}$  envelope proteins.

	Genotype lines	Mg-ATP	Mg-ATP + Co	Mg-ATP + Zn	Mg-ATP + Cu
<b>Measured ATPase activity</b> (%) as measured on highly purified chloroplast envelope fractions	WT	100±0.7	103±1.3	103 ±1.8	260 ±1.1
	<i>hma1</i> KO	63±8	66±6	79±12	204±5
	Ox	170±24	185±20	175±25	641±20
<b>Estimation of PAA1 (and other ATPases) activity</b> (%) as deduced from the specific activity measured in <i>hma1</i> mutants	WT	63±8	66±6	79±12	204±5
	<i>hma1</i> KO	63±8	66±6	79±12	204±5
	Ox	63±8	66±6	79±12	204±5
<b>Estimation of HMA1 ATPase activity</b> (%) as deduced from the total ATPase activity minus PAA1 and other ATPase activity	WT	37±8.7	37±7.3	24±13.8	56±6.1
	<i>hma1</i> KO	0	0	0	0
	Ox	107±30	119±26	96±37	437±25

**FIGURE 1**

**A**

MEPATLTRSSSLTRFPYRRGLSTLRLARVNSFSILPPKTLRQKPLRISASLSLPPRSIR  
 LRAVEDHHHDHHHDDEQDHHNHHHHHHQHGCCSVELKAESKPQKVLFGFAKAIGWVRLAN  
 YLREHLHLCCSAAAMFLAAAVCPYLAPEPYIKSLQNAFMIVGFPLVGVVSASLDALMDIAG  
 GKVNIHVLMAAFAFASVFMGNALEGLLLAMFNLAHIAEEFFTSRSMVDVKELKESNPDS  
 ALLIEVHNGNVPNISDLSYKSVPVHSVEVGSYVLVGTGEIVPVDCEVYQGSATITIEHLT  
 GEVKPLEAKAGDRVPGGARNLDGRMIVKATKAWNDSTLNKIVQLTEEAHSNKPKLQRWLD  
 EFGENYSKVVVLSLAI AFLGPF LFKWPF LSTAACRGSVYRALGLMVAA**SPC**ALAVAPLA  
 YATAISSCARKGILLKGAQVLDALASCHTIAFD**DKTGT**LTTGGLTCKAIEPIYGHQGGTNS  
 SVITCCIPNCEKEALAVAAAMEKGT**THP**IGRAVVDHSVGKDLPSIFVESFEYFPGRGLTA  
 TVNGVKTVAEESRLRKASLSIEFITSLFKSEDESKQIKDAVNASSYGKDFVHAALSVDQ  
 KVTLIHLEDQPRPGVSGVIAELKSWARLRVM**MLTGD**HDSSAWRVANAVGITEVYCNLKPE  
 DKLNVKNIAREAGGGLIMV**GE**GINDAPALAAATVGIVLAQRASATAIAVADILLRDNI  
 TGVPFCVAKSRQTTSLV↓**KQ**NVALALTSIFLAALPSVLGFVPLWLTVLL**HEGG**TLLVCLN  
 SVRGLNDPSWSWKQDIVHLINKLRSQEPTSSSSNSLSSAH-

**B**

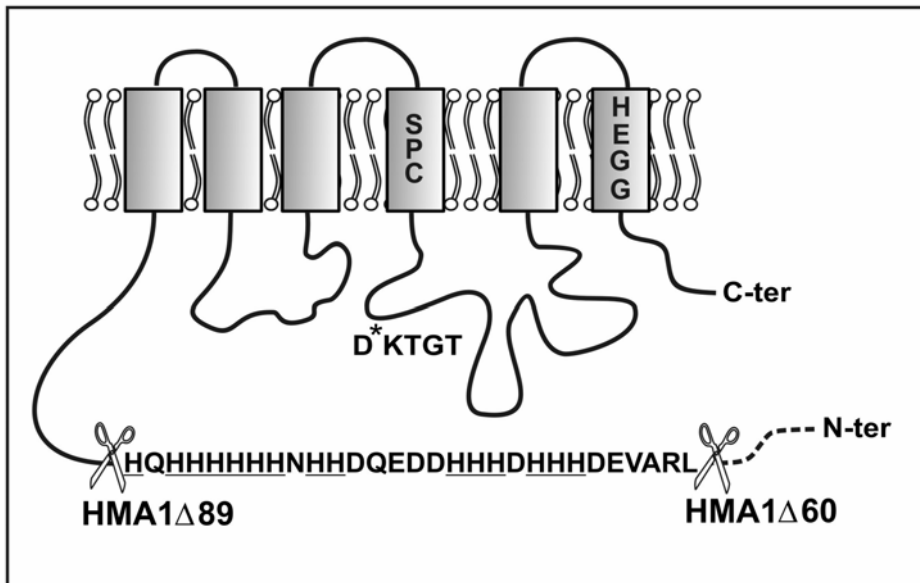


**FIGURE 2**

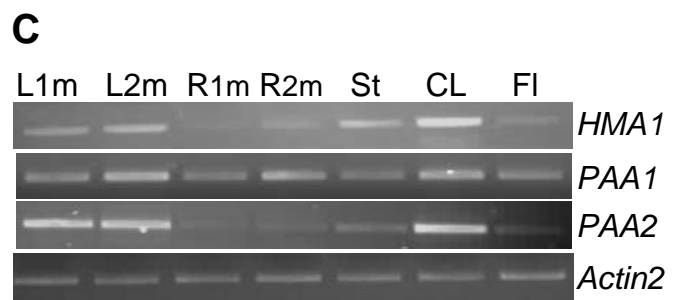
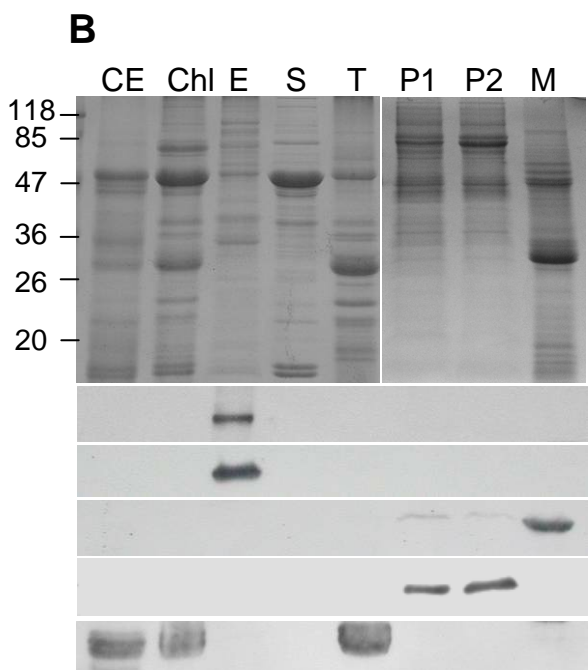
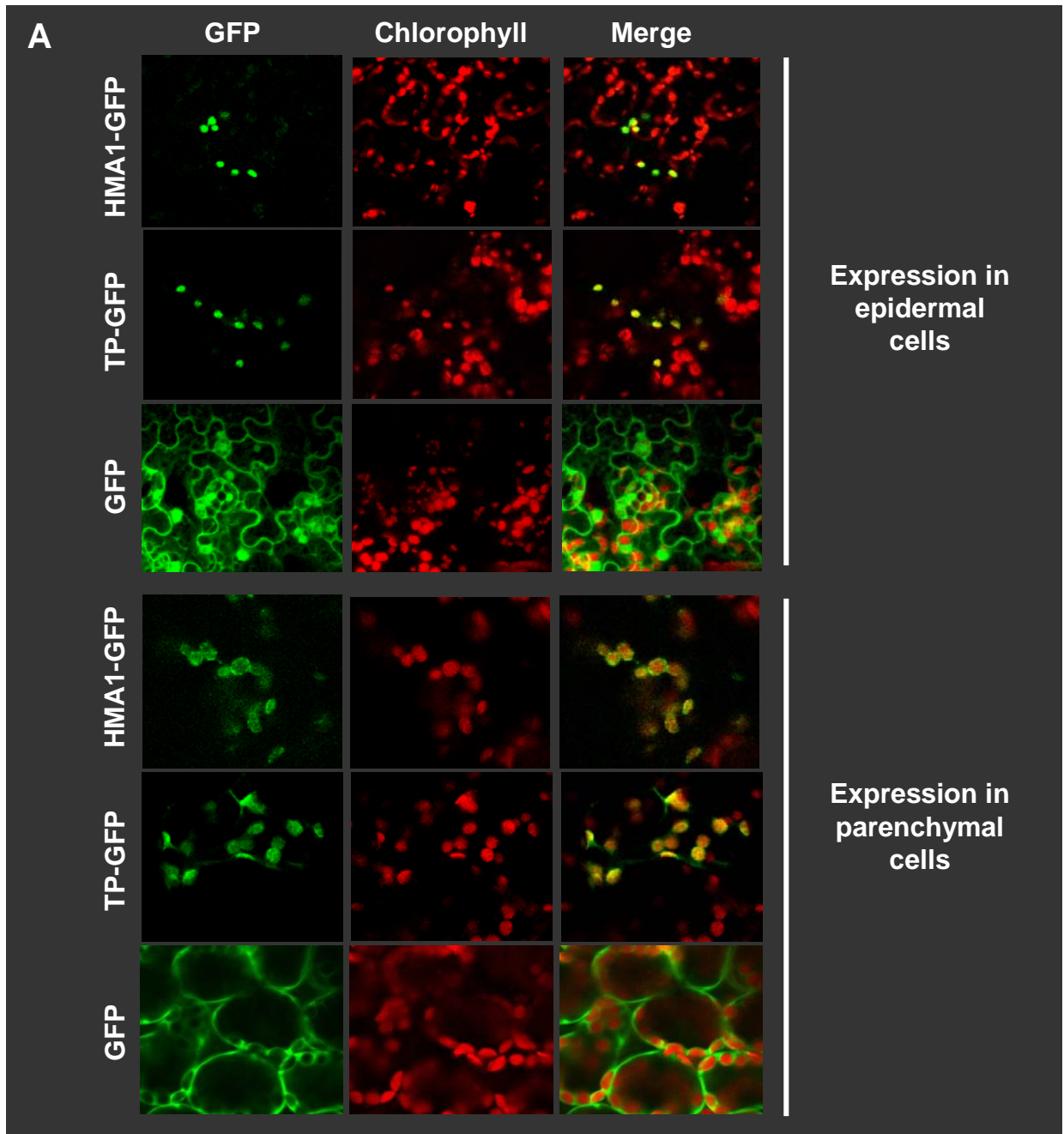


**FIGURE 3**

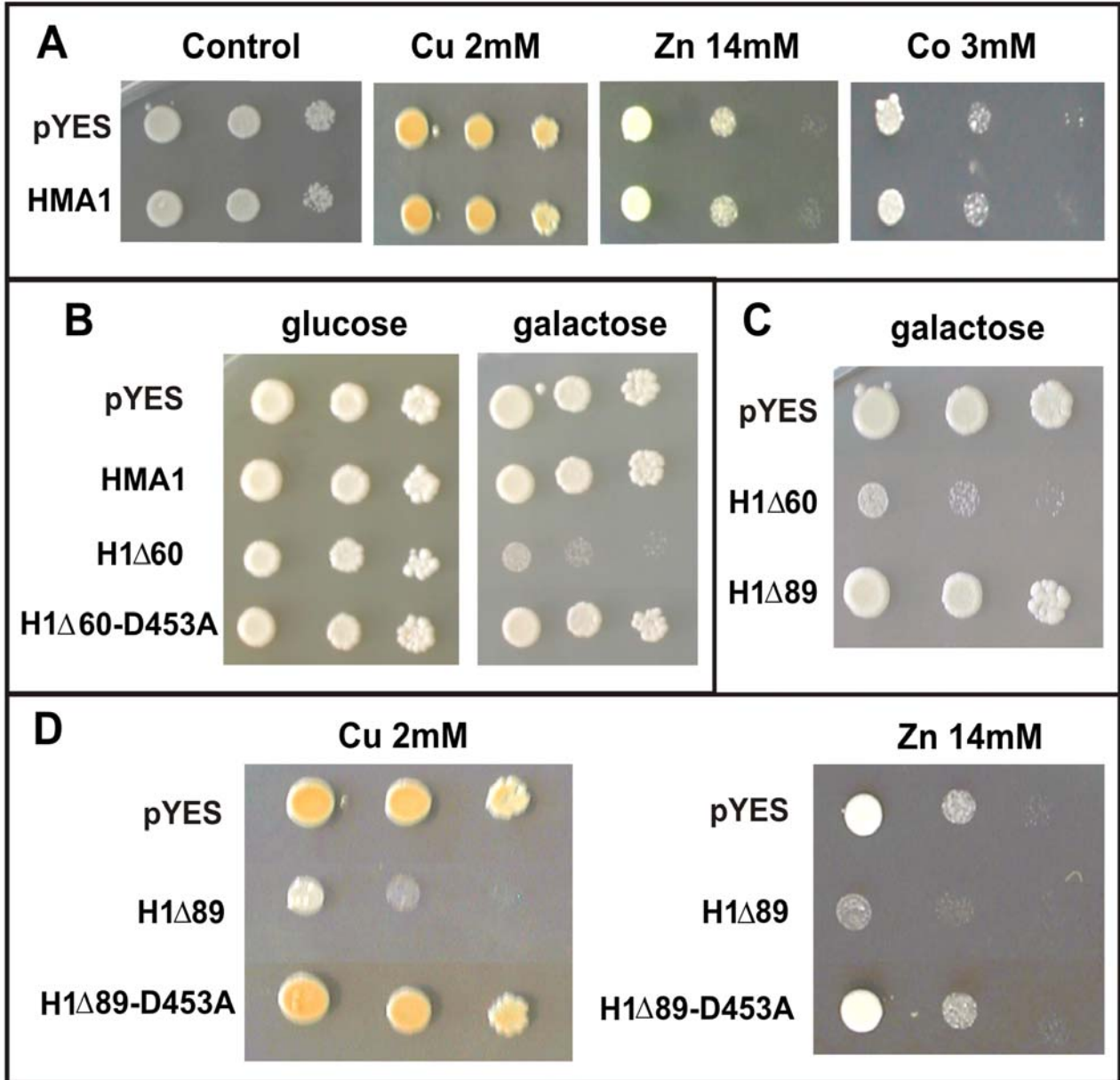


**FIGURE 4**

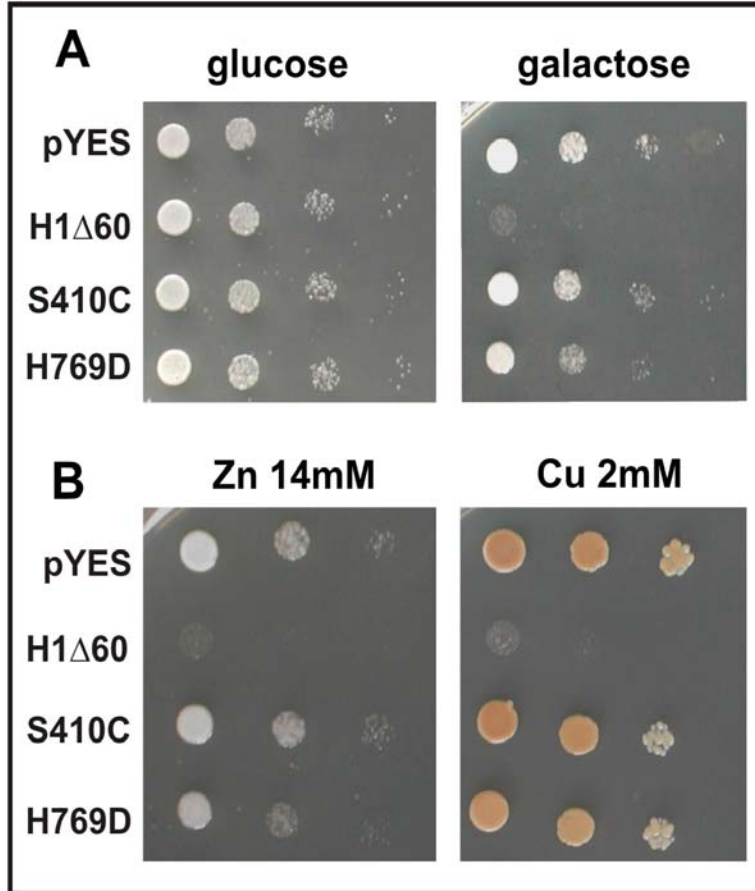


**FIGURE 5**

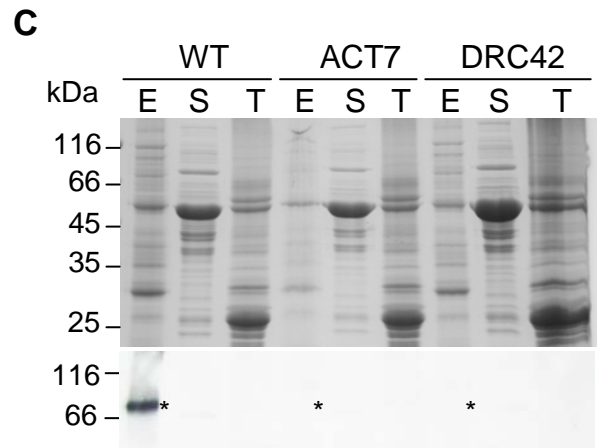
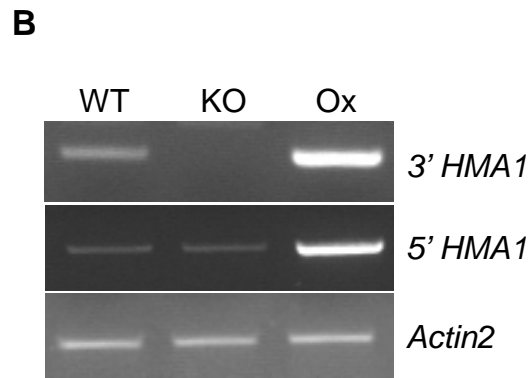
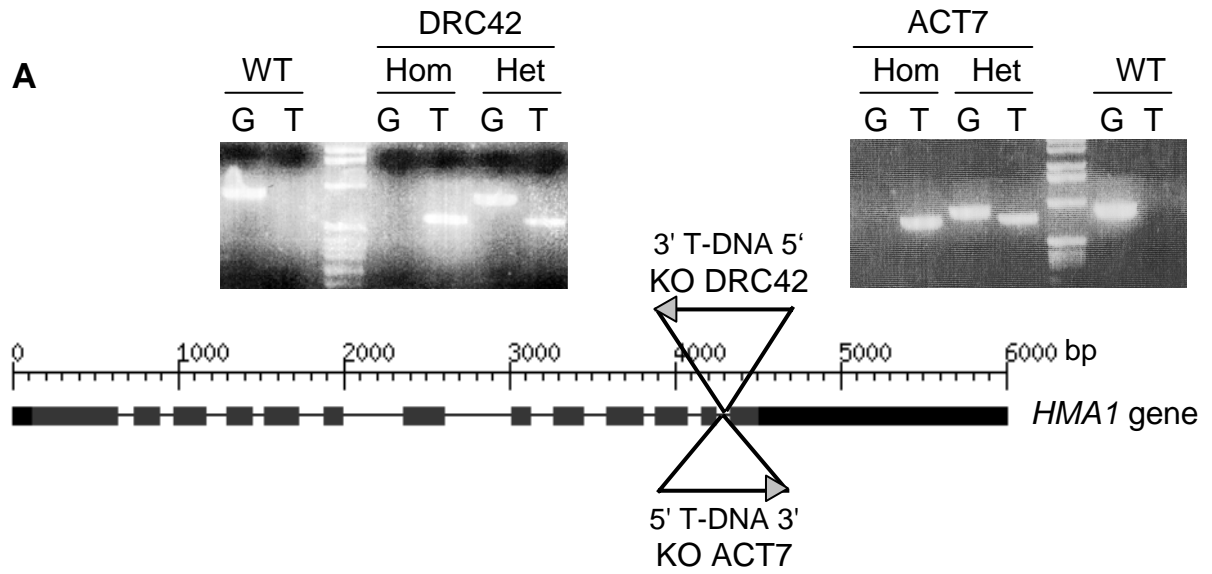


**FIGURE 6**

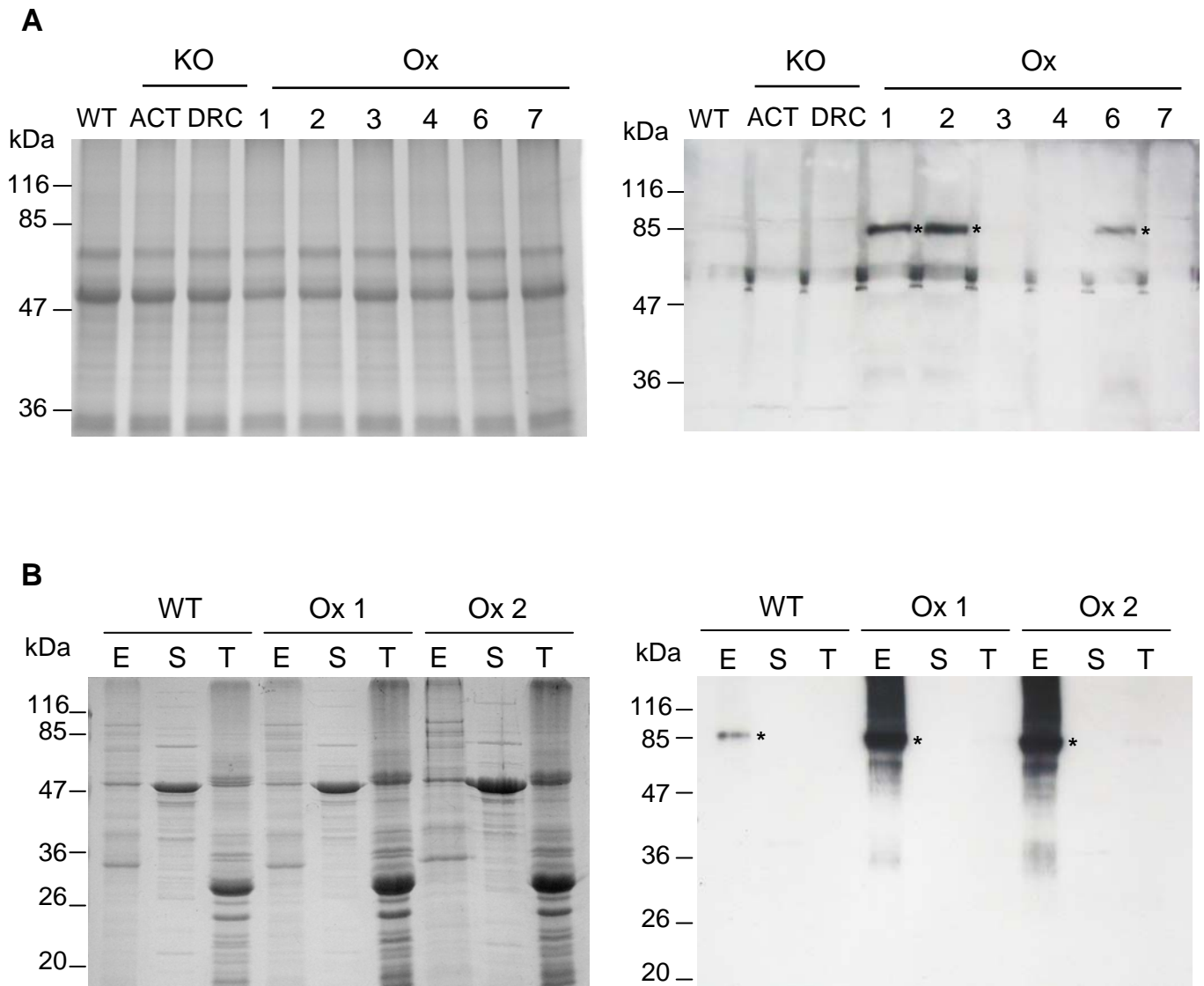
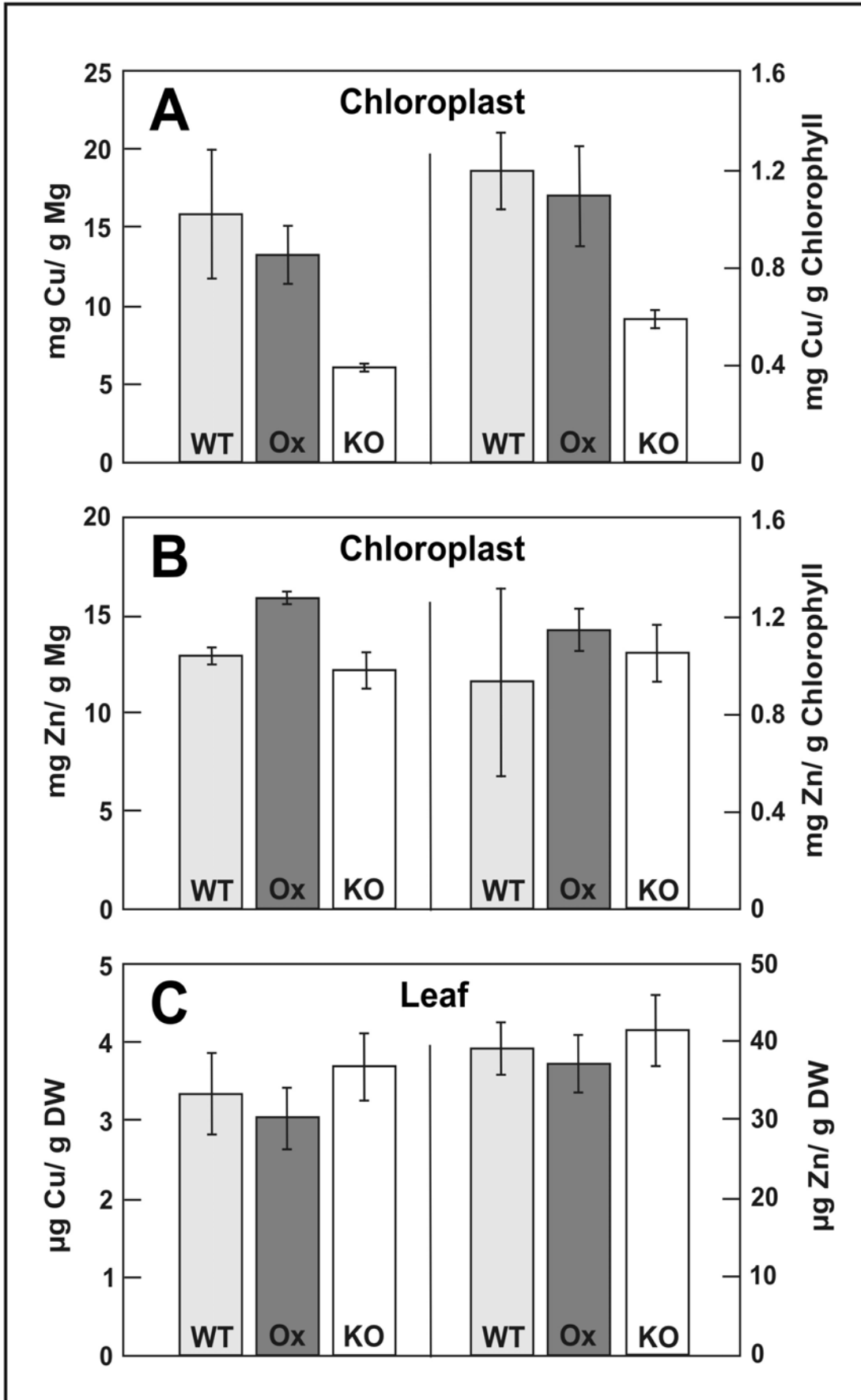
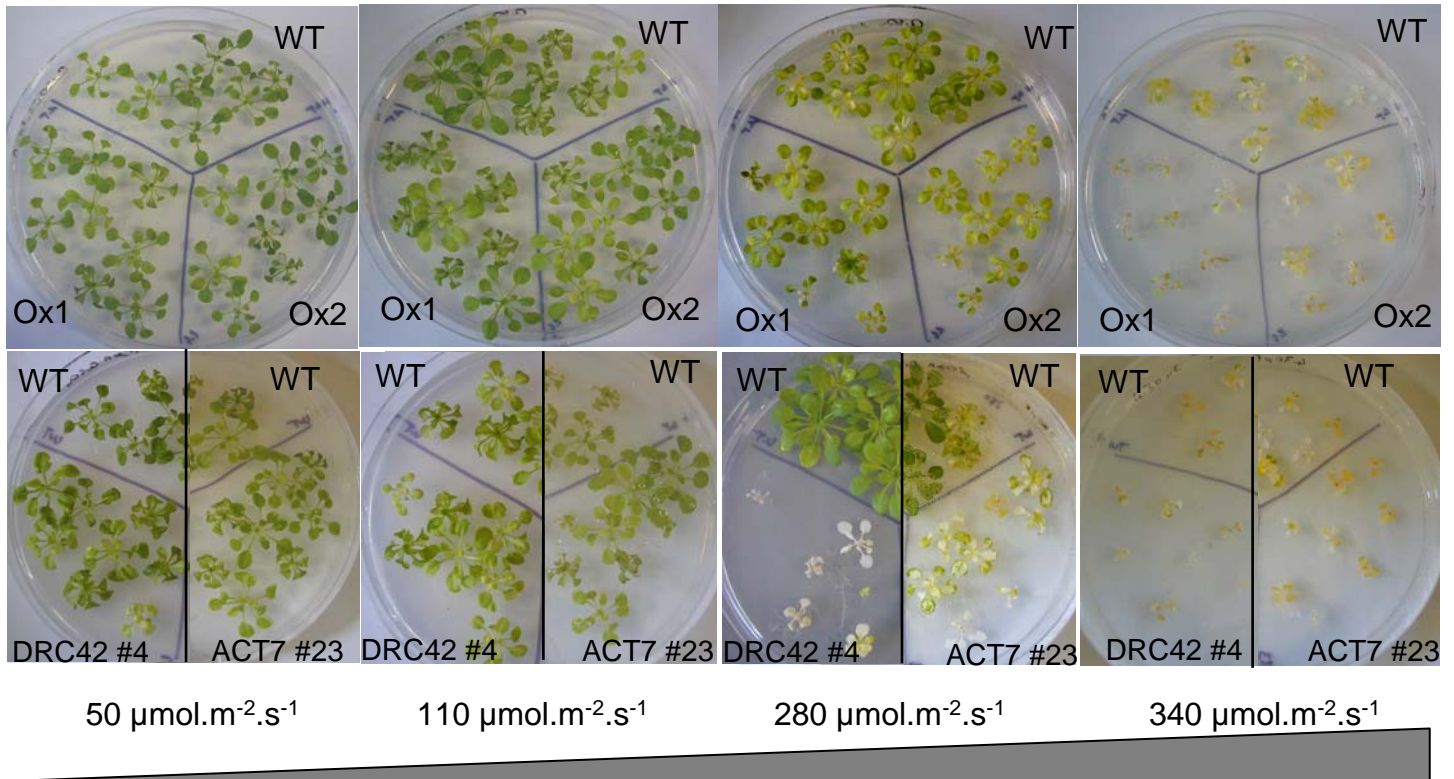


FIGURE 7

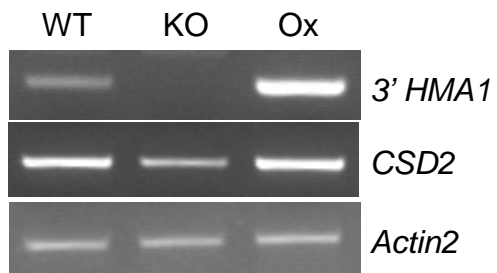


**FIGURE 8**

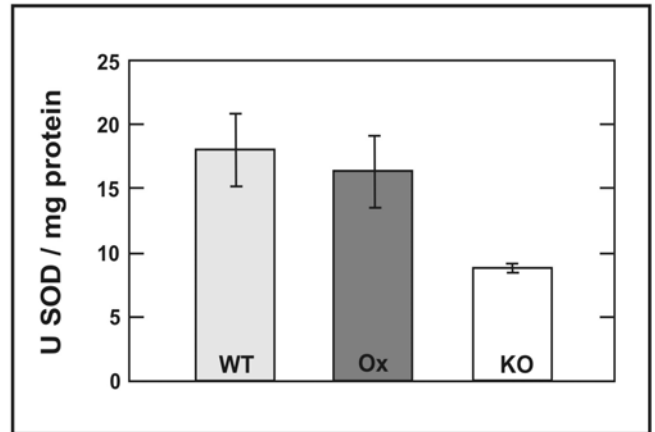


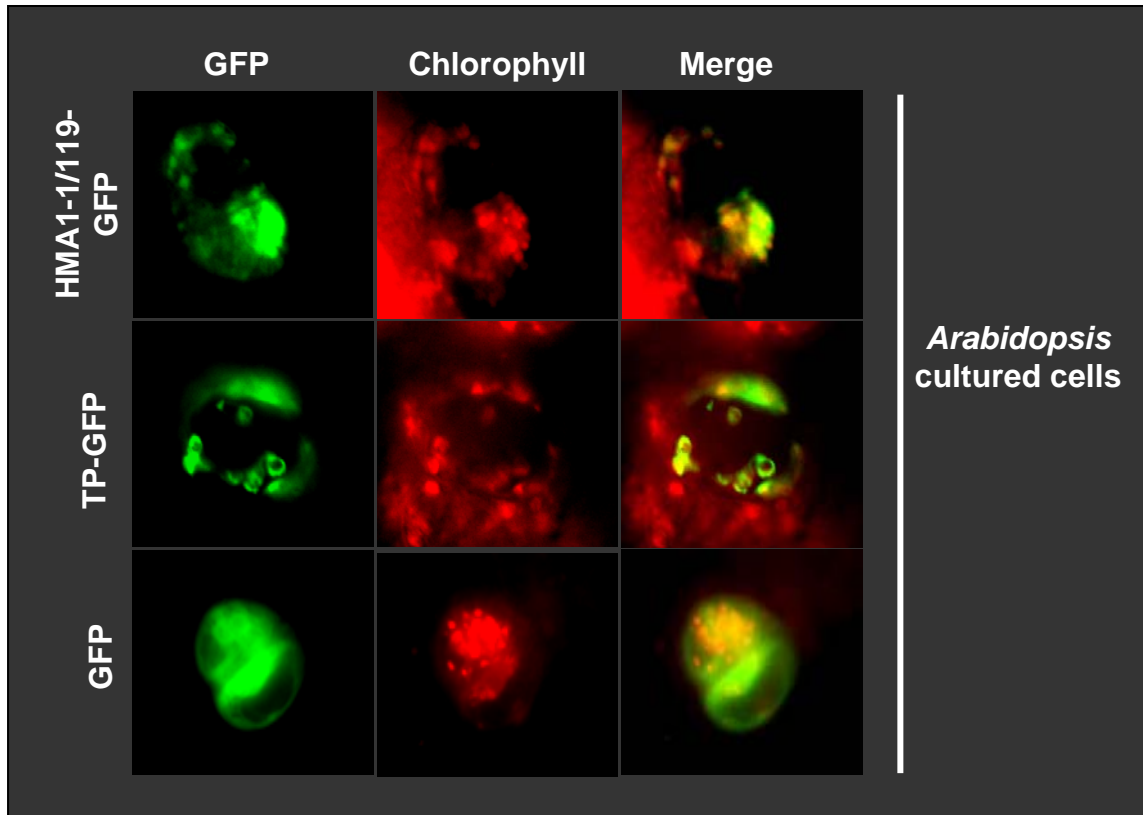
**FIGURE 9**

**A**



**B**

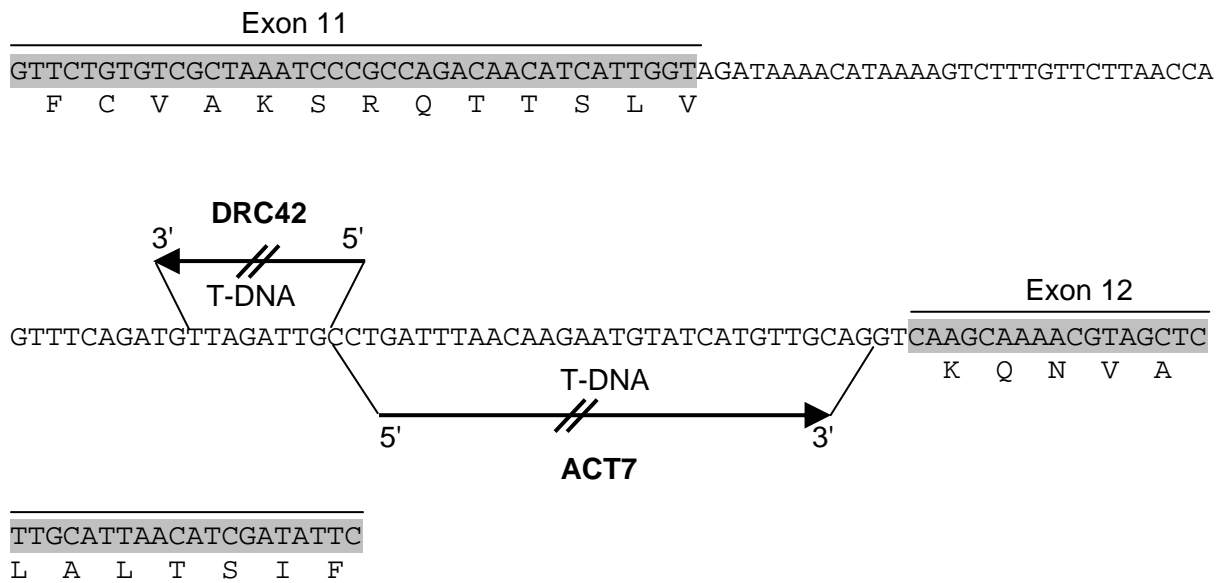




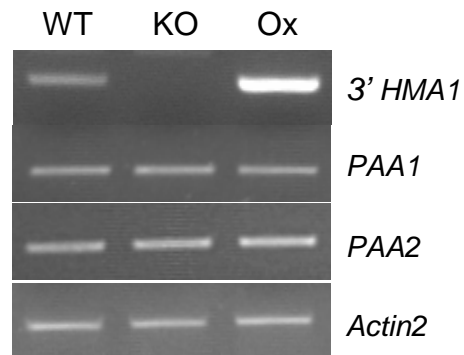
**Supplemental information 1.** Validation of the chloroplast localization of HMA1 by transient expression in *Arabidopsis* cultured cells. Localization of GFP and GFP fusions was analyzed in transformed cells by fluorescence microscopy. Transit peptide of the small unit of rubisco fused to GFP (TP-GFP) was used as positive control. Colocalization of GFP and chlorophyll fluorescences was observed for both the plastidial control TP-GFP and the HMA1-1/119-GFP fusion suggesting that HMA1 is a chloroplast protein.

*Construction of GFP reporter plasmids for transient expression in Arabidopsis* - Two plasmids were constructed to express HMA1 fused to GFP. The first one contains the entire sequence of *HMA1* and was obtained from PCR amplification with the primers *SalI*-N-ter (TTCGTCGACATGGAACCTGCAACTCTTACTCG) and *PciI*-C-ter (GCAACAGTTTAA GCTCTGCACATCACATGTGG). The second one (*HMA1-1/119*) contains only the N-terminal part of HMA1 (corresponding to aa 1 to 119) and was amplified from the same *A. thaliana* cDNA library using the primers *SalI*-N-ter (TTCGTCGACATGGAACCTGCAACTCTTACTCG) and *NcoI*-C-ter (GTCCATG GCCAATCTAACCCATCCG). Both PCR products were cloned into the pBluescript KS- vector (Stratagene). *SalI*-*PciI* or *SalI*-*NcoI* fragments were cleaved from these plasmids and inserted into the *SalI*-*NcoI* digested GFP reporter plasmid *Pro<sub>35S</sub>:sGFP(S65T)* to create the *Pro<sub>35S</sub>:HMA1-sGFP(S65T)* and *Pro<sub>35S</sub>:HMA1-1/119-sGFP(S65T)* vectors. The plasmids used for tissue bombardment transformation were prepared using the QIAfilter Plasmid Midi Kit (Qiagen Laboratories).

*Arabidopsis cells bombardment and fluorescence microscopy* - For transient expression of the proteins, plasmids of appropriate constructions (1 µg) were introduced into *Arabidopsis* cells using a pneumatic particle gun (PDS-1000/He; BIO-RAD). Growth of *Arabidopsis* cells, conditions of cell bombardment and fluorescence microscopy were as previously described (24).



**Supplemental information 2. Position of T-DNA insertions in *hma1* insertional lines ACT7 and DRC42.** PCR were carried out on genomic DNA using a primer for the T-DNA and a gene specific primer. The amplified bands were sequenced to confirm the T-DNA locations and orientations in *HMA1* gene.



**Supplemental information 3.** Expression of the chloroplast  $P_{1B}$ -type ATPases in WT plants, *hma1* mutant (KO; ACT7 #23) and HMA1 overexpressing plants (Ox 2). Expression profile of *HMA1*, *PAA1* and *PAA2* transcripts was determined by RT-PCR on RNA extracted from leaves of the various plants. *ACTIN2* transcript was used as a control. *3' HMA1*: amplification in the twelve and thirteenth exons, behind insertion of the T-DNA.